IN VIVO EXPERIMENTATION ON RAT INCISOR ENAMEL ORGANS THROUGH A SURGICAL WINDOW

by

MARC DOUGLAS McKEE

A thesis submitted to the Faculty of Graduate Studies and Research in partial fulfillment of the requirements for the Degree of Master of Science

Department of Anatomy
McGill University
Montreal, Canada.

Short Title

SURGICAL WINDOW ACCESS TO RAT INCISOR ENAMEL ORGANS

by

Marc Douglas McKee

Master of Science

ABSTRACT

Experimental agents administered systemically are costly and often toxic to animals. An in vivo technique has been developed whereby a surgical window in the alveolar bone allows selected areas of the rat incisor enamel organ and underlying enamel to be exposed to treatment with various drugs, molecular weight markers and radiolabeled molecules.

Sherman rats weighing 100gm were anesthetized and the inferior surface of each hemi-mandible was sugically exposed. A slow-speed dental hand drill was used to drill a small hole through the alveolar bone overlying the secretion zone of the enamel organ. The wound was closed and during recovery the mechanical trauma to the underlying tissue moved away from the hole due to the continuous eruption of the tooth. Two to five days later the hole was re-exposed and microinjections of ^{3}H-proline, ^{125}I-salmon calcitonin, vinblastine sulphate and normal saline (as control) were administered through the hole with a micromanipulator and microliter syringes. Radioautographic detection of ^{3}H-proline incorporation in secretory ameloblasts and enamel at 10 min., 30 min., 1 h and 4 h after injection was identical to that obtained previously by systemic injection. Two hours after microinjection of vinblastine sulphate the cellular response was again identical to that following systemic injection. ^{125}I-salmon calcitonin (MW~3600) was used as a molecular weight marker and was seen to diffuse into the enamel at 10 min. after injection. This study has demonstrated the feasibility of this new technique for experimentation on rat enamel organs.

Name: Marc Douglas McKee

Thesis Title: In vivo experimentation on rat incisor enamel organs through a surgical window.

Department: Anatomy

Degree: Master of Science **Date:** April, 1984

Résumé

Les produits expérimentaux administrés de façon systémiques sont couteux et souvent toxiques à l'animal. Nous avons mis au point une technique qui, en produisant une fenêtre chirurgicale *in vivo* dans l'os alvéolaire, nous permet d'exposer des régions sélectionnées de l'organe de l'émail et de traiter les tissues sous-jacent avec différentes drogues, marqueurs de poids moléculaire et molécules radioactives.

Des rats Sherman pesant 100 g ont été anesthésiés et la surface inférieure de chaque hémi-mandible a été exposée chirurgicalement. Un tour dentaire à vitesse lente a été utilisé pour percer un trou à travers l'os alvéolaire recouvrant la zone de sécrétion de l'organe de l'émail. La plaie a été refermée et, durant la période de guérison, la région de trauma mécanique s'est graduellement éloignée du trou à cause de l'éruption continue de la dent. De deux à cinq jours plus tard, le trou a été ré-exposé et des microinjections (~ .1 µL) de ^{3}H-proline, ^{125}I-calcitonine de saumon, sulfate de vinblastine et sérum physiologique (comme contrôle) ont été administrées à travers ce dernier à l'aide d'un micromanipulateur et des seringues micro-litre. La détection radioautographique de l'incorporation de ^{3}H-proline à 10 min., 30 min., 1 h et 4 h après l'injection était sembable à celle obtenue au paravant par injection systémique. Deux heures après la microinjection de sulfate de vinblastine la réponse cellulaire était également sembable à celle obtenue par injection systémique. La calcitonine marquée a l'^{125}Iode (poids moléculaire de 3600D) a été utilisée comme marqueur de poids moléculaire. Dix minutes après l'injection elle s'était diffusée à travers la couche d'émail. Cette étude démontre la faisabilité de cette nouvelle technique et son applicabilité à l'organe de l'émail chez le rat.

Nom: Marc Douglas McKee

Titre de la Thèse: Expérimentation sur l'Organe de l'Email de l'Incisive de Rat à l'Aide d'une Fenêtre Chirurgicale.

Département: Anatomie

Diplôme: Maîtrise en Sciences

Avril, 1984

To my parents

for their continuous support, love and encouragement

ACKNOWLEDGEMENTS

During the course of this study, the following persons were most helpful and to them I extend my sincerest thanks:

-to Dr. Y. Clermont for the opportunity of working in the Department of Anatomy.

-to Dr. Hershey Warshawsky for allowing me to pursue my interests by giving me the valuable opportunity of working in his laboratory. His warmth, patience and expert guidance made this rewarding learning experience most enjoyable.

-to Dr. Paul Bai whose experimental expertise and helpfulness originally motivated my work.

-to Ms. Darlene S. Mc Rae for her warm and unswerving friendship.

-to Drs. C.E. Smith, M. Lalli and J.J.M. Bergeron for numerous discussions.

-to Ms. K. Hewitt and Mr. F. Evaristo for their technical assistance.

-to Mr. A. Graham for his photographic assistance.

-to Mr. J. Khan for his animal assistance.

This work was supported through a grant from the Medical Research Council of Canada to Dr. H. Warshawsky.

TABLE OF CONTENTS

INTRODUCTION

INTRODUCTION

This study was undertaken in order to determine the feasibility of approaching the enamel organ of the rat incisor through the alveolar bone overlying the labial surface of the tooth. A technique using a slow-speed dental hand drill equipped with dental burs has been developed whereby a surgical window in the alveolar bone allows selected areas of the rat incisor enamel organ and underlying enamel to be exposed to microinjections of various drugs, radiolabeled molecules, and molecular weight markers. Experimental agents administered systemically are costly and often toxic to animals. The main objective of this study was to develop a microinjection technique in which minute amounts of experimental agents could be introduced through the surgical window in the alveolar bone and allowed to diffuse down and over selected areas of the enamel organ and underlying enamel. Subsequently, the fate and effects of microinjected experimental agents on the enamel organ and enamel of the rat incisor could be compared with the previously described effects of systemic injections of the same substance. A similar response of the enamel organ and enamel to the two different procedures would establish the feasibility of the microinjection technique.

DYNAMICS OF THE RAT INCISOR

The well-characterized dentition of the white laboratory rat was chosen for the application of this new technique. Specifically, the incisor of the rat has been shown to be an excellent model system in which to study the complex phenomena associated with amelogenesis (see reviews in Reith, 1960, 1961, 1963; Watson, 1960; Fearnhead, 1960, 1961a,b; Kallenbach et al., 1963; Warshawsky, 1968, 1971, 1978, 1979; Warshawsky and Smith, 1971, 1974; Weinstock and Leblond, 1971; Kallenbach, 1973;

Skobe, 1976; Warshawsky and Vugman, 1977; Smith, 1979; Leblond and Warshawsky, 1979). In the rat incisor, continuous attrition at the incisal end of the tooth is balanced by continuous production of dentin and enamel at the apical end of the tooth. More precisely, the odontogenic organ is responsible, either directly or indirectly, for the production of all the hard tissues of the tooth (Smith and Warshawsky, 1977).

Along the length of the incisor are several specialized cell populations. In a single well-orientated longitudinal section through the rat incisor, a continuous layer of ameloblasts can be seen on the labial surface of the tooth. This layer contains the entire sequence of developmental stages in enamel production and has been morphologically and functionally classified into several different zones of amelogenesis (Warshawsky and Smith, 1974). According to this classification, the entire length of the odontogenic and enamel organs is divided into the following zones: (1) Presecretory zone, (2) Secretory zone and, (3) Maturation zone. At the end of the maturation zone the ameloblasts become dramatically reduced in height and end their life as a desquamating cell around the gingival margin at the beginning of the erupted portion of the tooth. The proportion of time spent by the cells in each of these zones is proportional to the incisor length which they occupy, indicating that the cells' apparent migration rate is about the same at the various stages of their life cycle (Leblond and Warshawsky, 1979).

Renewal of the cell populations of the rat incisor was studied using ^{3}H-thymidine (Smith and Warshawsky, 1975). Radioautographically, it was established that a cohort of cells from each layer of the enamel organ is carried incisally with the erupting incisor and all of the cells in this cohort reach the gingival margin at the same time relative to their starting position. Previously, it had been reasoned that since these cells

make the hard tissues, they likely also move at a velocity which is similar to the rate of eruption (Ness and Smale, 1959; Starkey, 1963; Chiba, 1965; Hwang and Tonna, 1965). The study by Smith and Warshawsky (1975) concluded that "the true rate at which cells move and the rate at which the hard tissues move are equal. However, because there is growth in the length of the embedded portion of the incisor, the rate of cell migration, as measured relative to the zones of amelogenesis, appears to be faster than the rate of eruption (impeded), as measured in the oral cavity, and this difference is equal to the growth rate."

HISTOLOGY OF THE ENAMEL ORGAN-RELATED PERIODONTAL SPACE

The technique developed in this study involves penetration of the alveolar bone into the underlying periodontal space. The periodontal space consists of connective tissue that separates the growing incisor from the surrounding alveolar bone. At the lingual surface of the rat incisor, the connective tissue of the periodontal space forms the periodontal ligament (see review by Narayanan and Page, 1983). Related to the enamel organ at the labial surface of the tooth, the periodontal space contains connective tissue arranged differently from that of the periodontal ligament. This area was first described at the level of the light microscope by Matena (1972) and more recently its ultrastructure has been determined (Berkovitz and Shore, 1978a).

The general appearance of the connective tissue adjacent to the enamel organ is similar throughout the length of the tooth, although the width varies. Two zones may be distinguished within the connective tissue according to the density and shape of fibroblasts: (1) an inner enamel organ zone adjacent to the enamel organ in which the cells are elongated in both the longitudinal and transverse axes of the tooth and are com-

paratively numerous, (2) an outer alveolar zone where the cells are more round and sparse (Berkovitz and Shore, 1978a).

The enamel organ zone consists of several layers of elongated fibroblasts between which collagen fibrils are loosely arranged and orientated parallel to the long axis of the tooth (Berkovitz and Shore, 1978a). The fibroblasts show numerous organelles associated with protein synthesis: rER, Golgi saccules, and mitochondria. The cells also contain microtubules and microfilaments and their cell processes make contact with those of adjacent cells at desmosome-like junctions. The enamel organ zone also contains the extensive capillary network of the developing papillary layer.

The alveolar zone of connective tissue contains far fewer cells and collagen but noticeably more ground substance. The fibroblasts possess the intracellular organelles associated with protein synthesis and contain finely branching processes. Occasionally, collagen and single nerve fibers are encountered. No collagen fibers are inserted into the alveolar bone. Most striking is the abundance of venous sinuses that frequently almost completely occupy the alveolar zone. Latex casts (Kindlova and Matena, 1959) and longitudinal and cross sections of the incisor show the vessels to be arranged in a vascular network rather than a linear system. The network of venous sinuses in the alveolar zone is connected with the capillary network of the enamel organ zone at its margins opposite the mesial and lateral cemento-enamel junctions.

Comparatively, the reduced concentration, alignment and lack of insertion of collagen fibers is obvious in the enamel organ-related periodontal space relative to the periodontal ligament. The fibroblasts of both areas show considerable similarities with respect to general morphology. Also, in the alveolar zone of the enamel organ-related periodontal space, myelinated nerves occur mainly as single fibers, whereas in the periodontal

ligament they are more numerous and run in bundles (Berkovitz and Shore, 1978b).

The enamel organ-related periodontal space has been considered to supply a mechanical cushion, presumably hydrostatic in nature, protecting the growing tooth from injury (Kalninsh and Berzinsh, 1949).

THE ENAMEL ORGAN IN THE SECRETION ZONE

The microinjection technique developed in this study allows the secretion zone of the rat incisor enamel organ to be exposed to various experimental agents. The enamel organ in the secretion zone of amelogenesis consists of the developing papillary layer (outer dental epithelium and stellate reticulum), the stratum intermedium, and the ameloblast layer.

A basement membrane invests the basal aspect of the papillary layer, separating it from blood vessels and the connective tissue surrounding the enamel organ (Lehner and Plenk, 1936). The papillated outline of the enamel organ of the rat incisor was first described by Williams (1896). Reith (1959) described the papillae as a series of parallel ridges which extend across the enamel organ at right angles to the incisor axis. A network of capillaries separates the ridges of the papillary layer from each other (Kindlova and Matena, 1959; Adams, 1962; Garant and Nalbandian, 1968; Garant and Gillespie, 1969; Iwaku and Ozawa, 1979; Skobe, 1980). Between the capillaries, one or two rows of papillary cells overlie the stratum intermedium cells. The extracellular space is extensive in the papillary layer. Within the papillary cells, mitochondria are numerous and are disposed toward the connective tissue as well as lateral to the nuclei (Elwood and Bernstein, 1968). Endoplasmic reticulum is sparse and not confined to any particular region of the cell. The stratum inter-

medium cells form a layer one cell thick, adjacent to the proximal ends of the ameloblasts. These cells are smaller than the cells of the papillary layer, and their mitochondria are disposed lateral to the nuclei, toward adjacent stratum intermedium cells. The Golgi apparatus is located both above and below the nucleus. Vesicular structures are numerous in the cytoplasm towards the ameloblasts but endoplasmic reticulum is sparse.

The secretory cell of the enamel organ, the ameloblast, attains its maximal height in the enamel secretion zone. The cytoplasm of the ameloblast is subdivided into infranuclear, nuclear, supranuclear, and distal portions (Warshawsky, 1968). The infranuclear cytoplasm houses most of the cell's mitochondria (Watson and Avery, 1954), some rER, and the proximal junctional complex and cell web (Ronnholm, 1962). The supranuclear cytoplasm contains much rER orientated parallel to the long axis of the cell and an extensive tubular-shaped Golgi apparatus (Kallenbach et al., 1963). Smooth membrane vesicles, coated vesicles, secretion granules, lysosomes, and a few profiles of rough and smooth ER are present in the supranuclear cytoplasm (Warshawsky, 1968). Separating the distal cytoplasm from the supranuclear cytoplasm is an extensive cell web (Kallenbach et al., 1965) and distal junctional complex (Warshawsky, 1978). The distal cytoplasm of the secretory ameloblast is known as Tomes' process (Tomes, 1850) which is further subdivided into a proximal and interdigitating portion (Warshawsky, 1968). Tomes' process is devoid of organelles but contains free ribosomes, microtubules, coated vesicles and a core of secretion granules.

According to the classification of Warshawsky and Smith (1974), the secretion zone of amelogenesis may be subdivided into two regions: (1) region of inner enamel secretion and, (2) region of outer enamel secretion. The region of inner enamel secretion begins apically at the point of initial

enamel secretion and ends incisally at the point where Tomes' processes change from those typical of inner enamel secretion to those typical of outer enamel secretion. In the region of inner enamel secretion, the Tomes' processes incline slightly towards the apical end of the tooth. The cells engage in the production of rows of decussating enamel rods (Boyde, 1969; Warshawsky, 1971). The cell body of the ameloblast also appears slightly inclined. The stratum intermedium consists of a single continuous layer of cuboidal cells with large spherical nuclei. The organization of the discrete layer of stellate reticulum seen in the pre-secretion zone is lost in the secretion zone. The stellate reticulum and the outer dental epithelium are considered to collectively make up the developing papillary layer.

The region of outer enamel secretion begins at the limit of inner enamel secretion and ends incisally at the point where the interdigitating portion of Tomes' process disappears. The major change in this region is the thinning and lengthening of Tomes' processes and the increase in their angle of inclination towards the apical end of the incisor. The ameloblast body also inclines incisally to a greater extent than in the inner enamel secretion zone. These ameloblasts produce rods which do not decussate. The papillary layer increases in height and regularity and the thickness of the enamel layer increases.

RADIOAUTOGRAPHIC STUDIES OF AMELOGENESIS

In order to demonstrate the applicability of the microinjection technique to radioautographic studies, ^{3}H-proline, a labeled amino acid precursor of the organic matrix of enamel, was microinjected over the enamel secretion zone of the rat incisor. The organic matrix of enamel is almost exclusively composed of proteins and radioautography has been used

to identify the sites of synthesis of these proteins and their ultimate destinations in the enamel organ and enamel of the rat incisor (Warshawsky, 1966). The synthetic pathway of enamel matrix proteins has now been elucidated (Weinstock and Leblond, 1971; Leblond and Warshawsky, 1979; Warshawsky, 1979).

Radioautographic analysis of the secretory process in ameloblasts has shown that enamel proteins are synthesized entirely within the ameloblast cytoplasm as early as 10 min. after injection of ^{3}H-proline (Warshawsky, 1966). The radioactive proteins are rapidly secreted as a layer of enamel at 30 min., and this layer of labeled enamel increases in width at 1 and 4 h after injection. At later time intervals, the labeled enamel proteins progressively spread from the initial site of deposition and become homogeneously dispersed throughout the entire layer of enamel. The process in which recently formed enamel proteins intermix with previously formed matrix is called randomization (see review in Leblond and Warshawsky, 1979), and its significance is not known. Therefore, the ameloblast is the site of synthesis of enamel matrix proteins. These proteins are rapidly secreted and can migrate throughout the previously formed enamel.

INFLUENCE OF VINBLASTINE SULPHATE ON SECRETORY AMELOBLASTS

In order to demonstrate the potential of the microinjection technique for administering experimental agents that alter cell function and morphology, vinblastine sulphate was microinjected over the enamel secretion zone of the rat incisor. The vinka alkaloid vinblastine sulphate has been shown to disrupt microtubules (Ekholm et al., 1974; Ericson, 1980; Williams, 1981), and to interfere with secretion (Redman et al., 1975; Ericson, 1980; Williams, 1981). Vinblastine binds to the microtubule subunit tubulin, preventing polymerization, and results in a loss of micro-

tubules (Dustin, 1978). Secretory activity of the ameloblast is severely altered after systemic injection of vinblastine (Moe and Mikkelsen, 1977; Takuma et al., 1982; Nanci, 1982), and similar results were also obtained with colcemid (Karim and Warshawsky, 1979; Nishikawa and Kitamura, 1982). Microtubules are absent and the organization of intracellular organelles is altered. In particular, secretory granules are no longer seen in Tomes' process, and instead, ectopic secretion sites are observed between ameloblasts. Therefore, vinblastine is frequently used as a biological tool to elucidate the role of microtubules in various types of cells.

IN VIVO EXPERIMENTATIONS ON RAT INCISORS

Previously, many methods of in vivo experimentation on rat incisors have been implemented. Surgical manipulations such as root resections and transections (Berkovitz and Thomas, 1969; Berkovitz, 1971) have convincingly implicated the periodontal ligament to be directly or indirectly associated with the mechanism of the eruption of the tooth. These procedures involve surgically removing a portion of the mandibular alveolar bone and wounding or removing the underlying dental tissues. Other ways of penetrating the alveolar bone have been developed (Melcher, 1970; Gould et al., 1977). These procedures consist of drilling a hole through the alveolar bone to the level of the periodontal ligament in mouse molars in order to stimulate and locate progenitor cells of the periodontal ligament.

PURPOSE AND ORIGINALITY OF THIS STUDY

With surgical manipulation in mind, this study was undertaken in order to determine the feasibility of approaching the enamel organ of the rat incisor through the alveolar bone overlying the labial surface of the tooth. This thesis describes an in vivo experimental procedure which has been developed to approach the enamel organ of the rat incisor. The

feasibility of this new technique is compared and contrasted to the conventional method of systemic injection.

This is the first attempt to utilize such a system to explore problems in amelogenesis. Using this new technique, microinjections of ^{3}H-proline were localized radioautographically and show an identical pathway of incorporation into the enamel matrix as that seen after systemic injection. Microinjection of vinblastine sulphate caused morphological and functional changes in ameloblast structure again identical to those produced by systemic injection. This study has also demonstrated the permeability of the enamel matrix to relatively large molecular weight substances as shown by the diffusion of ^{125}I-salmon calcitonin into the enamel matrix at 10 minutes after microinjection. Furthermore, this study has demonstrated the susceptibility of the enamel to trauma following mechanical breakthrough of the alveolar bone surrounding the tooth. This may have important clinical significance during surgical procedures involving the mandible or maxilla in children with developing dentition.

MATERIALS AND METHODS

MATERIALS AND METHODS

ANIMALS AND TISSUE PROCESSING

Sherman and Sprague Dawley rats weighing approximately 100gm were used in this study. The animals were anesthetized with intraperitoneal injections of Nembutal and sacrificed by perfusion through the left ventricle with lactated Ringer's solution (Abbott) for 30 sec. followed by perfusion for 10 min. with an aldehyde mixture consisting of 2% acrolein and 2.5% glutaraldehyde in 0.05M sodium cacodylate buffer, pH 7.3. The mandibles were dissected and immersed in the above fixative for 4 h at 4°C followed by washing in 0.1M sodium cacodylate buffer containing 0.05% $CaCl_2$, pH 7.3. The mandibles were then decalcified in 4.13% isotonic, neutral disodium EDTA (Warshawsky and Moore, 1967) and were cut into segments that were extensively washed in the above 0.1M sodium cacodylate buffer. The incisor segments were subsequently post-fixed in 2% osmium tetroxide for 4 h at 4°C, dehydrated in graded acetone and embedded in Epon 812.

LIGHT AND ELECTRON MICROSCOPY

Each segment was orientated for sectioning along the long axis of the incisor. One μm thick sections were cut with glass knives on a Reichert Om U2 ultramicrotome and stained with toluidine blue. Thin sections (gold interference color) were cut with a diamond knife, mounted on copper grids and stained with uranyl acetate (Watson, 1958) for 5 min. and lead citrate (Reynolds, 1963) for 3 min. Sections were examined with either a Siemens Elmiskop IA or a Siemens 101 at 80KeV. Sections used for light microscope radioautography were placed on a hot plate prewarmed to 80 C,

flooded with a mordant solution of 5% ammonium sulfate for 10 min., rinsed in distilled water and replaced on the hot plate. They were then flooded with Regaud's 1% hematoxylin for 1 min. and again rinsed in distilled water. Sections were differentiated with tap water for 3 min. followed by a last rinse in distilled water. The sections were then coated with Kodak NTB2 emulsion and exposed for various time intervals (Kopriwa and Leblond, 1962).

DRILLING TECHNIQUE

Animals were anesthetized with an intraperitoneal injection of Nembutal and the inferior surface of each hemi-mandible was surgically exposed. Retractors were used to hold back the musculature and the area was kept moist with rinses of physiological saline. A slow-speed dental hand drill equipped with a straight handpiece and carbide dental burs was used to drill a small hole through the alveolar bone overlying either the secretion or maturation zones of the enamel organ (Fig. 1). Complete penetration through the alveolar bone into the vascular periodontal space overlying the enamel organ was determined by tactile sensation and immediate bleeding upon breakthrough. The bur was removed and gauze was placed over the hole for 1 min. to stop the bleeding and the area was again rinsed with physiological saline. In animals that were sacrificed within 10 min. after drilling, the wound was kept moist, but open. At longer time intervals the wound was closed and during recovery the mechanical trauma to the underlying dental tissues moved away from the hole due to the continuous eruption of the tooth.

Recovery from trauma

In order to follow the recovery and repair of mechanical trauma

caused by the drill, hemi-mandibles of 12 animals were surgically exposed and the alveolar bone was drilled as described above. A 1/4-round carbide dental bur was used and each hemi-mandible was drilled in the alveolar bone overlying the secretion zone of the enamel organ. The animals were sacrificed at 0 h, ½ h, 2 d, and 5 d after drilling, by intracardiac perfusion and the tissues were processed. Longitudinal sections of the incisor were cut so as to include, in the same plane of section, both the original hole in the alveolar bone and the area of trauma to the underlying dental tissues that had moved away from the hole due to the continuous eruption of the tooth into the oral cavity.

Experimental application of heat

In an attempt to simulate local frictional heat generated by the drill, two animals were used in which the drilling procedure was carried out as described above with the exception that only a small, shallow pit was drilled into the alveolar bone with no penetration into the periodontal space. A similar bur was heated to "red-hot" in an open flame and was immediately placed into the pit of the original drill site for approximately the same time it takes to drill a hole completely through the alveolar bone. The animals were sacrificed immediately by intracardiac perfusion and prepared for sectioning as described above.

Bur configuration

Animals were prepared for drilling as described above with the exception that the burs used to penetrate the alveolar bone to the level of the periodontal space were of different size, shape and blade configuration. The various burs were obtained from Beaver Dental Products, Ltd. and their variations are shown in Fig. 2. Furthermore, a hand-held dental reamer

was slowly rotated between two fingertips, and in this manner, was used to penetrate the alveolar bone. The animals were immediately sacrificed by intracardiac perfusion.

MICROINJECTION TECHNIQUE

Animals were drilled in the alveolar bone overlying the secretion zone of the enamel organ. The wound was closed and during recovery the mechanical trauma to the underlying tissue moved away from the hole by the continuous eruption of the tooth. Two to five days later the hole was re-exposed to permit microinjections as described below.

Description of microinjection apparatus

A vertical compact micromanipulator (Brinkmann Instruments, Model MM 33) was mounted on a column stand and a micrometer (Scherr-Tumico, Inc.) was inserted into its clamping mechanism to allow for extremely fine vertical movements of a microsyringe plunger (Fig. 3). One hundred microliter microsyringes were obtained from the Hamilton Co. (Cat. No. 710) and were fitted with 33 gauge luer lock needles. A rubber band was used to keep the plunger of the syringe firmly applied to the plunger of the micrometer. In this way, small amounts of the solution to be injected were drawn into the syringe by the micrometer. Graduations on the micrometer were calibrated to the graduations on the syringe which allowed dispensing of accurate, reproducible, minute volumes of solution.

Microsyringe procedures

Due to the small bore size of the 33 guage needles used in this study, several precautions had to be taken to insure accurate and consistent microinjections. The needle tip was filed down from its original

bevel to a flat surface using 600 grade emory cloth. Both microsyringe and needle were thoroughly rinsed with physiological saline, rapidly plunged to remove any compressible air bubbles, and the plunger was slowly withdrawn so as to partially fill the syringe with a "buffer zone" of saline. The syringe was then mounted to the micromanipulator. Solutions could now be drawn into the syringe of the micromanipulator assembly. The syringe was filled only immediately prior to injection and paraffin film was used to seal the tip of the needle between injections to prevent evaporation of the solution from the small bore diameter at the tip of the needle.

Microinjection of ^{3}H-proline

L(2,3-^{3}H) proline (specific activity 32.2 Ci/mmol) was purchased in 0.01N HCl (New England Nuclear). Under a stream of nitrogen gas, 0.1 ml of solution containing 100 μCi of ^{3}H-proline, was evaporated to dryness. The amino acid was redissolved in 1 μl of physiological saline to provide for ten injections of 0.1 μl containing 10 μCi of ^{3}H-proline. The solution then slowly was drawn into the microsyringe. Two days prior to microinjection, a minimum of 20 animals were drilled in the alveolar bone overlying the secretion zone of the enamel organ in both hemi-mandibles and allowed to recover. The holes were then re-exposed and the tip of the needle was lowered approximately 0.5 ml into the connective tissue plug that had filled the lesion in the bone. Approximately 0.1 μl of solution containing 10 μCi of ^{3}H-proline was microinjected under a dissecting microscope into the right hemi-mandible. The needle was withdrawn immediately, the solution was allowed to "sink in" for 2 min., and the wound was closed. The left hemi-mandibles were not injected. Animals were sacrificed at 10 min., 30 min., 1 h, 4 h, 1 d, and 2 d after micro-

injection, by intracardiac perfusion. The tissues were processed for radioautography.

Microinjection of vinblastine sulphate

A group of five rats was drilled in both hemi-mandibles as above, two days prior to microinjection. The right hemi-mandibles were microinjected with 0.1 µl of a stock solution of 5 mg/0.30 ml saline of vinblastine sulphate (Sigma). Injections of physiological saline into the left hemi-mandibles served as controls. All animals were sacrificed by intracardiac perfusion two hours after microinjection.

Microinjection of ^{125}I-salmon calcitonin

Synthetic salmon calcitonin (sCT); approximately 2500 mU/µg, was iodinated with isotopic sodium iodide (Na ^{125}I); specific activity 17 µCi/mg (New England Nuclear), by the Chloramine T method described by Hunter and Greenwood (1962). Following these procedures the supernatant containing the ^{125}I-sCT (M.W.~3600D) was subsequently evaporated to dryness under a stream of nitrogen gas and redissolved in 2.5% (w/v) bovine serum albumin in 25 mM TRIS-HCl buffer, pH 7.4. From this solution, 0.1 µl was microinjected into the right hemi-mandibles of two 100gm rats drilled in the alveolar bone overlying the maturation zone 2 d prior to injection, and the animals were sacrificed by intracardiac perfusion 10 min. thereafter. The tissues were processed for radioautography.

ANALYSIS OF THE PERIODONTAL SPACE

Five Sherman rats weighing approximately 100gm were anesthetized and sacrificed by perfusion as described above. After decalcification, a segment containing the inner enamel secretion zone, corresponding to the

drill site of the previous experiments, was dissected from the right hemimandible of each animal. The segments were washed in 0.1M sodium cacodylate buffer, post-fixed in 2% osmium tetroxide, dehydrated in graded acetone and embedded in Epon. One μm-thick sections were cut in the longitudinal axis of the incisor and stained with toluidine blue.

The tissues related to the enamel aspect of the incisor were divided into the following compartments: (1) bone, consisting of the alveolar prebone and bone but not including adjacent periosteum and endosteum, (2) periodontal space, consisting of the connective tissue between the alveolar bone and the developing papillary layer, (3) enamel organ, consisting of the entire enamel organ including the capillaries of the developing papillary layer but excluding the interdigitating portion of Tomes' process found therein and, (5) venous sinus, consisting of the venous sinuses found within the periodontal space. These compartments are outlined in Figure 3.1.

One histological section from each of the five animals was selected for this study. A rectangular area was superimposed over the compartments related to the zone of inner enamel secretion (Fig. 3.1). The rectangular area was orientated so that its length was perpendicular to the enamel. Within each rectangular area, the relative area and thickness of each compartment to the total compartmental area and thickness was measured using a Zeiss MOP-3. The thickness of each compartment was determined by measuring along the border of the rectangle closest to the apical end of the tooth. Three adjacent rectangular areas (a,b,c) in the inner enamel secretion zone were measured in each animal.

RESULTS

RESULTS

DEFINING THE LESIONS

Drilling through the alveolar bone of the mandible causes trauma to the underlying dental tissues that moves incisally away from the drill site due to the continuous eruption of the tooth. Figure 4 shows the trauma and its incisal movement two days after drilling. The dental tissue trauma appears as an altered or ruptured enamel organ overlying a complete discontinuity in the enamel layer. This discontinuity extends completely through the enamel to the dentino-enamel junction. The bone lesion at the drill site is seen as a hole in the alveolar bone filled with a plug of connective tissue. A "healthy" region of enamel and enamel organ has been passively carried underneath the bone lesion due to the eruption of the tooth (the large arrow indicates the direction of tooth eruption). Note the vascularity of the region between the enamel organ and the alveolar bone, the periodontal space (Fig. 4).

Alveolar bone lesions

The bone lesions are seen in histological sections as prominent interuptions of the alveolar bone. Figures 5 and 6 show two lesions drilled over the enamel secretion zone in which the animals were sacrificed two days after drilling. The enamel lesions have moved incisally and "healthy" enamel and enamel organ has advanced underneath the drill site. The cut edges of bone are clearly visible and bone fragments occasionally surrounded by cells resembling osteoclasts may be observed. Bleeding often occurs into the connective tissue of the periodontal space and extends laterally from the drill site. Normal vascular channels traversing the

the alveolar bone are numerous and lined by osteoblasts. Occasionally, the drilling will cause a "bone flap" to hang down in a manner that compresses the enamel organ as it moves past the flap during eruption (Figs. 7,8). The enamel organ appears to "squeeze" underneath the flap but incisally loses its normal morphology. Only on two occasions did drilling of the alveolar bone not cause trauma to the enamel or enamel organ. In both examples, the hemi-mandibles were drilled over the enamel secretion zone, complete penetration of the alveolar bone was achieved, and the animals were sacrificed immediately (Figs. 9,10). The drilling occured directly over a vascular sinus in the periodontal space and there was no rupture of the endothelium on the side facing the enamel organ.

Electron microscopy shows that bone fragments caused by the drilling may be lined with active osteoclasts (Figs. 11,12). These osteoclasts were multinucleated, contained numerous mitochondria, and showed the characteristic clear and ruffled zones suggestive of bone resorption. These cells also may be found lining the cut edges of the bone lesion. Frequently found within the connective tissue plug of the bone lesion are osteoblast-like cells, filled with distended rER and surrounded by numerous, small collagen fibrils (Fig. 13). Osteoblasts also are found frequently lining the cut edges of the bone lesion (Fig. 14).

Enamel and enamel organ lesions: Light microscopy

Drilling of the labial alveolar bone in the rat hemi-mandible almost invariably causes lesions in the enamel organ and the underlying enamel. The lesions presumably occur when the drill bur penetrates the alveolar bone and plunges a short distance into the periodontal space. Animals sacrificed immediately after drilling (0 h) exhibited the same degree of trauma as those lesions in which the animals were sacrificed up to 5 days

after drilling. Figures 15 and 16 show lesions at 0 h in which the enamel and enamel organ have been completely stripped from the dentin. In most cases, the dentin shows no sign of trauma (Figs. 16-19). The enamel organ of the lesions in which the enamel is completely stripped from the dentin may be ruptured and display a "gushing" effect (Figs. 15,16), or may be completely intact for the extent of the lesion (Figs. 17-19). In the latter case, serial sections show the enamel organ to be ruptured at some point over the enamel lesion. Fragments of enamel may be seen at some distance from the enamel layer (Fig. 16) and occasional remnants of enamel may be seen at the dentino-enamel junction (Fig. 18).

Animals sacrificed at 12 h after drilling show similar enamel lesions (Figs. 20,21). Remnants of enamel remain at the dentino-enamel junction and many red blood cells are present at the site of the lesion. The ameloblasts have been torn away from the enamel, their nuclei are pyknotic, and they show signs of degeneration. Rod profiles are readily apparent in the remaining enamel and the spaces between them seem exagerated.

At 2 d post-drilling the enamel lesions have moved incisally approximately one millimeter. This corresponds to the normal rate of tooth eruption (Smith and Warshawsky, 1975). Figures 22 and 23 show enamel completely removed at the dentino-enamel junction, the dentino-enamel junction is unscarred, and clusters of red blood cells are seen at the lesion site. Note that the vasculature of the periodontal space remains relatively intact (Fig. 22). The lesion in Figure 24 again shows a typical accumulation of blood, a ruptured enamel organ, and lack of enamel. Furthermore, several new features of the lesion become apparent. At the dentino-enamel junction and extending only as wide as the lesion, can be seen a thin layer of dark-staining material. This material is not present where enamel completely covers the dentin. At the periphery of the lesion, an amorphous

dense material frequently is observed between ameloblasts and may appear as small globules or long, extensive accumulations (Fig. 24). Also at the periphery of the lesion, apposed to the ragged edges of the enamel, are cells of unknown origin which appear to be in intimate contact with the enamel. Figures 25 and 26 show a lesion at 2 d post-drilling that was drilled in the outer enamel secretion zone and has since moved into the enamel maturation zone. This lesion shows what appears to be smooth-ended ameloblasts extending over the ragged edge of the enamel at the periphery of the lesion. These cells still show intimate contact with the enamel. Separated rod profiles are apparent and cells may be seen to "creep" between the enamel and the dentin where the enamel is slightly torn away. Figures 27 and 28 again show similar features. The cells lining the dentino-enamel junction may be derived from the enamel organ as the capillary network of the papillary layer may be followed over the lesion. The cells resemble stratum spinosum or stratum intermedium cells. The dark-staining material again is seen at the dentino-enamel junction. At the periphery of the lesion (Figs. 28,29) the enamel thickness is constant, indicating an inhibition of secretion due to the trauma. Ameloblasts have decreased in height but Tomes' processes appear intact. Accumulations of red blood cells, singly stacked or packed in oval clusters not bound by endothelium, are found between ameloblasts. These accumulations conform to the spatial limitations of the ameloblast layer.

Lesions at 5 d post-drilling show features similar to those at 2 d post-drilling (Figs. 30,31). A gross preparation of an animal sacrificed 24 d after drilling is seen in Fig. 1. Bone remodeling has occurred at the drill site and the erupted enamel lesion appears as a shallow pit. The distance between the bone lesion and the enamel lesion corresponds to the normal eruption rate over a 24 day period.

Enamel and enamel organ lesions: Electron microscopy

At the periphery of the lesion, red blood cells were frequently found between ameloblasts (Figs. 32,33). Their presence did not seem to disrupt the normal morphology of the ameloblasts but some displacement of ameloblasts may have occurred(this feature is seen light microscopically in Figs. 28,29). Red blood cells were also observed in the periodontal space (Fig. 34).

Also at the periphery of the lesion but apposed to the ragged edges of the enamel, were cells exhibiting a wide range of morphological characteristics of which several trends were noted. Figure 35 shows a mononuclear cell, with mitochondria and a moderate amount of rER, apposed to the enamel surface. The cell membrane follows the irregular contour of the enamel surface and possesses junctional specializations with neighboring cells (Fig. 36). Observed between two cells of this type is an amorphous, homogeneous, light-staining material (Figs. 35,37). Higher magnification shows these accumulations to be either of a granular nature (Figs. 38,40,41) or homogeneously dense (Fig. 39; corresponds to the black arrow in Fig. 24). The lighter-staining substance is not always present, but the cells frequently show finger-like projections into the intercellular space (Figs. 40,41).

Another cell type often seen apposed to enamel at the periphery of the lesion is shown in Figures 42-44. These cells are osteoclast-like in appearance and possess clear zones and numerous mitochondria characteristic of osteoclasts. They have finger-like projections into the intercellular space but otherwise, the cell membrane follows the irregular surface of the enamel. Occasionally seen within the clear zone are membrane bound structures containing what appears to be enamel (Fig. 43).

Figures 45-47 show cells closely apposed to the enamel surface. In all cases, mitochondria are numerous. A ruffled border may be present (Fig. 46)

or simple cytoplasmic extensions may interdigitate with the enamel (Figs. 45,47). Higher magnifications of membrane-enamel relationships (Figs. 48-50) show vacuolar and vesicular structures within the cytoplasm. These structures and their contents are occasionally continuous with the plasma membrane and are therefore exposed to the enamel (Figs. 49,50). Membrane-bound granules, similar to the secretion granules of ameloblasts, are sometimes observed (Fig. 50). Also, coated pits, desmosomes, and other junctional specializations are frequent (Fig. 47).

The enamel at the periphery of the lesion presents one of several abnormal morphologies (Figs. 51-54). Generally, rod profiles appear separated (corresponds to the white arrows in Figs. 20,26) and frequently a lightly granular or filamentous material is dispersed between the rod and interrod enamel. Occasionally, rods may be delineated only by sheaths of greater density at their periphery (Fig. 53).

Also associated with the enamel at the periphery of the lesion are amorphous dense globules (Figs. 55-57). These globules are most frequently seen at the rod-interrod interface or are seen within the lightly granular material mentioned above. These same globules may also be seen in close association with membrane remnants (Figs. 58-62). Most frequently, the globules are aligned between the membrane and the enamel but sometimes may be completely enclosed by membrane.

Frequently seen within the enamel at the periphery of the lesion are amoeboid cells "crawling" through the separations of rod and interrod enamel (Figs. 63,64). These cells have a prominent Golgi apparatus, relatively little rER, and an abundance of lysosomes. Accumulations of lipid droplets frequently are observed. Similar cells are seen at the dentino-enamel junction (Figs. 65,66; corresponds to the black arrow in Fig. 26).

At the center of the lesion the enamel has been completely removed. In its place, at the dentino-enamel junction, an amorphous layer of material can be seen (Figs. 67-72). This layer completely covers the dentin, may vary in thickness, and extends to the periphery of the lesion where enamel again overlies the dentin (corresponds to the white arrows in Figs. 24,28). At higher magnification this layer seems to be bounded by two zones of increased density(Fig. 71). In all cases, the arrangement of collagen fibrils in the dentin is abnormal at the dentino-enamel junction since the irregular interdigitations of initial enamel and dentin normally seen, are not present.

EFFECTS OF HEAT AND BUR CONFIGURATION

The procedure for application of heat to the alveolar bone (Materials and Methods) did not cause any trauma to the underlying dental tissues. Animals sacrificed immediately after the "red-hot" bur was placed in the drilled pit in the alveolar bone showed a completely intact enamel organ and enamel (Figs. 73,74). However, leucocytes and red blood cells were numerous at the drill site.

Drill burs of different size, shape and blade configuration used to penetrate the alveolar bone all caused equal degrees of trauma to the underlying dental tissues. Figures 75 and 76 are two examples of the trauma caused by two different burs. The lesions may be characterized in the same way as the lesions previously described in which the animals were sacrificed immediately after drilling (0 h). The enamel organ is torn away from the enamel, the enamel is completely removed from the dentin, and the dentin at the dentino-enamel junction remains undamaged. All the drill burs in Figure 2 caused similar lesions.

The hand-held dental reamer used to penetrate the alveolar bone, did

not cause any trauma to the underlying enamel organ or enamel.

RADIOAUTOGRAPHIC LOCALIZATION OF ^{3}H-PROLINE

The microinjection technique allowed small amounts of ^{3}H-proline to be introduced into the right hemi-mandible over the enamel secretion zone. The labeled amino acid was then utilized by the secretory ameloblasts and incorporated into all proteins being synthesized at that time, including the enamel matrix proteins. At 10 minutes after microinjection, silver grains were located over the supranuclear region of the ameloblasts (Fig. 77). By 30 minutes, the distribution of the label in the supranuclear zone was unchanged from above, but in addition, a reaction band was seen over Tomes' processes of the ameloblasts (Fig. 78). At 1 hour after microinjection the reaction band over Tomes' processes had greatly intensified. Silver grains were still found over the supranuclear zone (Fig. 79). By 4 hours, fewer grains were found over the supranuclear zone and the reaction band in the enamel was deeper into the enamel (Fig. 80). At 1 day the reaction was seen over the entire depth of the enamel but stopped at the dentino-enamel junction (Fig. 81). Some silver grains were still observed over the ameloblasts. By 2 days after microinjection, grains were still seen over the entire enamel layer but very few were seen over ameloblasts, which were now ameloblasts of outer enamel secretion (Fig. 82).

Frequently, ^{3}H-proline entered the bloodstream after microinjection. This was observed as a reaction band in the predentin at 4 hours in the uninjected contralateral left hemi-mandible (Fig. 83) in the same animal as the injected right hemi-mandible shown in Figure 80. Figure 84 shows an intense radioautographic reaction over cells in the connective tissue plug at the drill site 1 day post-microinjection. Osteoblasts lining

vascular channels in the alveolar bone also are labeled heavily. Silver grains are seen over the entire thickness of the enamel and as a band over the calcification front of the dentin.

RADIOAUTOGRAPHIC LOCALIZATION OF ^{125}I-salmon CALCITONIN

^{125}I-salmon calcitonin microinjected into the right hemi-mandible over the early maturation zone was localized by radioautography 10 minutes after microinjection (Fig. 85). Most striking was the reaction observed over the entire thickness of the enamel. Silver grains were found in greater density in the outermost enamel but nevertheless extended completely over the enamel up to the dentino-enamel junction. The dentin only showed background labeling. Labeling also was seen over the ameloblasts and over the periodontal space, but to a lesser extent over the papillary layer.

EFFECTS OF VINBLASTINE SULPHATE

Microinjection of vinblastine sulphate into the right hemi-mandible over the enamel secretion zone of the rat incisor, caused numerous disruptions of normal morphology of the secretory ameloblasts. The organization of organelles within the ameloblasts was disrupted (Figs. 86-93). The infranuclear zone contained mitochondria, rER, and numerous secretion granules (Figs. 86,87). Occasionally, Golgi saccules were seen in this region (Fig. 88). Figure 87 shows the linking of several secretion granules by a continuous membrane. In the supranuclear zone, marked accumulations of granules were seen (Figs. 89-91) and these were clustered around the stacks of Golgi saccules (Fig. 90). Rough endoplasmic reticulum appeared fenestrated or fragmented . Patches of a granular, dark-staining

material were seen between ameloblasts (Figs. 89,91). Tomes' processes also showed significant alterations in normal morphology. The interdigitating portion of Tomes' process was completely devoid of organelles (Figs. 92,93). Although a few membrane infoldings were found, they were not as frequent as in controls. A tubular network was sometimes observed in Tomes' process (Fig. 92) and coated pits also were seen (Fig. 93). Microinjection of physiological saline served as controls and these animals showed normal ameloblast morphology.

THE PERIODONTAL SPACE

The relative areas of the labial periodontal and dental compartments to the total compartmental area in the inner enamel secretion zone of the mandibular incisor are shown in Table I. Similar areas were measured among the experimental animals. The alveolar bone compartment occupies the largest relative area.

The relative thickness of each of the compartments to the total thickness in the inner enamel secretion zone is shown in Table II. Note that the combined relative thickness of the periodontal space and the enamel organ approximately is equal to the relative thickness of the alveolar bone.

DISCUSSION

DISCUSSION

This study has demonstrated a new technique whereby the formation of a surgical window in the labial alveolar bone of the rat hemi-mandible allows the underlying enamel organ and enamel of the incisor to be exposed to microinjections of various experimental agents. The application of this procedure to the well-characterized dental tissues of the rat incisor has been used to address some of the problems concerning the complex phenomena of amelogenesis.

RESPONSE OF THE ENAMEL ORGAN AND ENAMEL TO DRILLING PROCEDURES

In the early stages of this work, it was noted that complete penetration of the labial alveolar bone of the rat incisor by a carbide dental bur attached to a slow-speed dental hand drill, almost invariably caused trauma to the underlying enamel organ and enamel in the zone of enamel secretion. This trauma occurred as a ruptured enamel organ and complete removal of the enamel up to the dentino-enamel junction (Figs. 15-31). Immature enamel taken from the zone of enamel secretion is often referred to as "cheesy-enamel" and contains about 30% organic matrix by weight (see review in Leblond and Warshawsky, 1979). Massive net selective loss of enamel matrix proteins occurs at a fairly specific stage of development at or shortly after the full thickness of the tissue has been laid down (Robinson et al., 1977, 1978, 1981). It is not clear how the organic matrix is removed. Penetration of the alveolar bone overlying the enamel secretion zone by drilling causes complete removal of enamel underneath the drill site up to the dentino-enamel junction (Figs. 15-31). This indicates that the enamel in the secretion zone is relatively soft and

can be disturbed by nearby turbulence such as that caused by the drill bur. The more rigid matrix of the dentin remains intact and undamaged along the entire length of the lesion.

Several possibilities as to the cause of the trauma were investigated. Superficially, it would appear that the enamel lesion was the result of the bur coming in contact with the enamel layer, indicated by the ruptured enamel organ and by the shape and extent of enamel loss. However, several histological features of the lesion and the experimental techniques employed argue against this possibility. Firstly, complete penetration of the alveolar bone by the bur almost invariably produces identical lesions of the enamel organ and enamel. In each of these lesions, the enamel layer is entirely removed yet the dentin at the dentino-enamel junction remains completely undamaged. If the bur had come into contact with the relatively thin layer of enamel, inevitably the bur would occasionally also come into contact with the dentin. Lesions which were created purposefully by allowing the bur to descend to the level of the enamel and dentin show dentin which is damaged or completely ruptured by the bur as shown in Figure 94. This possibility is not supported by the consistent reproducibility of identical enamel lesions in which the layer of dentin remains unscarred and intact along the entire length of the lesion. Secondly, at the periphery of the lesion, there may be a complete loss of enamel, yet the integrity of the enamel organ persists (Figs. 17-19) and the dentin remains undamaged. Although serial sections show the enamel organ to be ruptured at some point over the central region of the lesion, the loss of enamel underlying an intact enamel organ may not be explained by the penetration of the bur into the enamel. Thirdly, the use of a slow-speed hand drill was chosen so as to allow good tactile sensation in the hands of the investigator. During the course of this study, the drilling procedure was

performed on a minimum of 100 animals in which repetition of the technique allowed the exact moment of breakthrough of the alveolar bone to be determined. This breakthrough also coincided with moderate bleeding after rupture of some of the venous sinuses in the alveolar zone of the periodontal space. The bur immediately was withdrawn following tactile sensation of breakthrough and the appearance of blood. In a further attempt to clarify this issue, measurements of relative area and length were made of the tissue compartments in this area (Tables I,II). The results indicate that after complete penetration of the alveolar bone, in order for the bur to reach the enamel layer, it would have to traverse a distance equal to the combined thickness of the periodontal space and enamel organ compartments, which is greater than the thickness of the alveolar bone compartment. It is highly unlikely that the tactile sensation felt upon breakthrough of the alveolar bone would include a "followthrough" that would extend the distance to the enamel layer, a distance greater than that needed to penetrate the alveolar bone. For these reasons it was concluded that the enamel lesion is caused by factors other than contact with the drill bur.

The heat generated by the frictional interface between the bur and the alveolar bone was considered suspect in causing the lesion. This possibility was investigated by placing a "red-hot" bur in a previously drilled shallow pit in the alveolar bone, for the same time interval that it takes to drill a hole completely through the alveolar bone (Figs. 73,74). This procedure applies heat far in excess of any frictional heat generated by the drilling. In these experiments, although empty osteocyte lacunae and ruptured vascular channels were seen in the alveolar bone, no enamel lesions were found, thus indicating that frictional heat does not cause the enamel lesions.

Another experimental parameter considered suspect in causing the

enamel lesions was the size, shape and blade configuration of the bur. To investigate this possibility, different burs were used to penetrate the alveolar bone (Fig. 2). In all cases, these burs caused similar enamel lesions (Figs. 75,76). In an attempt to minimize any turbulence caused by a rapidly rotating drill bur, a hand-held dental reamer was slowly rotated between two fingertips, and in this manner, was used to penetrate the alveolar bone. Complete penetration of the alveolar bone using the hand-held dental reamer did not cause any trauma to the underlying enamel organ and enamel.

The results of this study suggest that the drill bur, after complete penetration of the alveolar bone, descends a relatively short distance into the connective tissue of the periodontal space. At this point the bur immediately is withdrawn. However, during the short period of time that the bur is actually within the periodontal space it is rapidly spinning, and this motion may be sufficient to cause turbulence within the tissues of the periodontal space that is transduced to the enamel organ and enamel, resulting in the enamel lesion. The histological appearance of the lesion suggests that a portion of enamel directly below the rotating bur is "torn" away from the enamel layer.

The lesion occurs immediately after drilling of the alveolar bone (Figs. 15,16) and presumably undergoes repair as evidenced by the appearance of lesions in which the animal was sacrificed at later time intervals after drilling (Figs. 17-71). At the periphery of the lesion, cells show intimate contact with the ragged edges of the enamel (Figs. 35-37, 45-50), accumulations of a dark-staining material, similar in nature to the organic matrix of enamel, are seen between cells (Figs. 35-41) and amoeboid cells are seen between separated rod and interrod enamel (Figs. 63-66). Ameloblast-like cells apposed to the enamel may show signs of secretory or

resorptive activity (Figs. 42-50). Red blood cells may accumulate between these ameloblasts (Figs. 27-29,32,33), indicating a nearby rupture of at least the proximal junctional complex. Centrally, where the enamel has been completely stripped away, the lesion is characterized by an amorphous layer of material at the dentino-enamel junction (Figs. 67-72). This may represent an adsorption of local, non-specific proteins to the exposed dentin.

Routine thin sections and freeze-fracture replicas of secretory ameloblasts reveal a proximal and distal junctional region associated with a moderate proximal cell web and an extensive distal cell web (Kallenbach et al., 1965; Warshawsky, 1968, 1978). The cells of the developing papillary layer in the secretion zone also are characterized by frequent junctional contacts (Kallenbach, 1967; Elwood and Bernstein, 1968). The trauma caused by the drilling frequently tears the enamel organ away from the enamel (Figs. 17-19). At the periphery of the lesion, the enamel organ may be torn from the enamel yet maintain its organizational integrity. This elasticity presumably results from the numerous junctional contacts within the enamel organ. This feature again is demonstrated by the ability of the enamel organ to "squeeze" beneath an interfering bone flap produced by the drilling procedure (Figs. 7,8) as the enamel organ is carried incisally by the eruption of the tooth into the oral cavity.

APPLICATIONS OF THE MICROINJECTION TECHNIQUE

The microinjection technique described in this study has demonstrated a new in vivo approach to experimentation on rat incisors. ^{3}H-proline and vinblastine sulphate were successfully microinjected over the enamel organ and enamel of the secretion zone of the mandibular rat incisor, and gave results identical to those following systemic injection. In some circum-

stances, the microinjection technique has several advantages over the method of systemic injection. Firstly, experimental agents that are toxic to animals when administered systemically may be microinjected over selected areas of the enamel organ and enamel, and the animal may be sacrificed at any time thereafter. Secondly, in the continuously growing incisor of the rat, a cohort of cells in the enamel organ and the underlying enamel matrix, at any specific developmental stage of amelogenesis, may be selectively exposed to various experimental agents. Furthermore, due to the incisal eruption of the tooth, the evolution of this same cohort and its underlying enamel, and the fate and effects of the previously administered experimental agents, may be followed as they pass through the different developmental zones of amelogenesis. Thirdly, systemic administration of radiolabeled molecules requires that they be injected in quantities high enough to reach, through the bloodstream, all the tissues of the body. Frequently, a dose of 1000μCi of a radiolabeled molecule is administered systemically to a 100gm animal. The purchase or production of such radiolabeled molecules is costly. Using the microinjection technique, only 10μCi of label, 1/100th of that necessary for systemic injection, is introduced to a small, selected volume of cells thereby eliminating the unnecessary distribution of radioactivity to other tissues of the body.

Vinblastine sulphate and ^{3}H-proline were selected as representatives of a drug and a radiolabeled molecule, respectively, to assess the feasibility of the microinjection technique. When administered systemically, vinblastine disrupts microtubules (Ekholm et al., 1974; Ericson, 1980; Williams, 1981) and interferes with secretion (Redman et al., 1975; Ericson, 1980; Williams, 1981). The results are identical to those produced by colcemid (Karim and Warshawsky, 1979; Nishikawa and Kitamura, 1982). The ameloblasts lose their intracellular organization of organelles, marked accumul-

ations of secretion granules are present, ectopic secretion sites are observed between ameloblasts, Tomes' processes are devoid of organelles and relatively few membrane infoldings are associated with the rod and interrod enamel growth sites (Moe and Mikkelsen, 1977; Takuma et al., 1982; Nanci, 1982). Vinblastine sulphate, microinjected by the technique developed in this study, caused identical alterations in the morphological appearence and functional activity of the secretory ameloblast. These results demonstrate the feasibility of administering drugs by the microinjection technique.

When administered systemically, ^{3}H-proline is utilized by the secretory ameloblast and incorporated into the organic matrix of enamel (Warshawsky, 1966; Weinstock and Leblond, 1971; Leblond and Warshawsky, 1979; Warshawsky, 1979). Enamel proteins are synthesized within the ameloblast cytoplasm as early as 10 minutes after injection, are secreted as a layer of enamel at 30 minutes, and this layer of labeled enamel increases in width at 1 and 4 hours to eventually become homogeneously dispersed throughout the entire layer of enamel in a process termed randomization (see review in Leblond and Warshawsky, 1979). ^{3}H-proline microinjected by the technique developed in this study, follows identically the same synthetic pathway and incorporation into the enamel matrix. These results demonstrate the feasibility of administering radiolabeled molecules by the microinjection technique.

When a single injection of ^{3}H-proline is administered intravenously, the labeled amino acid rapidly circulates to capillaries and within minutes appears in the tissues of the animal. When the animal is sacrificed and the tissues processed for radioautography, the unused labeled amino acid that may still be present is washed out, while the labeled protein is retained within the tissue. Presumably, a similar route of entry of ^{3}H-pro-

line into the enamel organ and enamel follows after microinjection. ^{3}H-proline is microinjected into the connective tissue plug that results from the drilling procedure. The labeled proline rapidly diffuses to the ameloblasts of the enamel organ as demonstrated by radioautographical localization of labeled proteins at 10 minutes after microinjection (Fig. 77). Once the amino acid has reached the level of the connective tissue surrounding the capillary network of the enamel organ, presumably it behaves and is utilized by the enamel organ in the same manner as amino acids diffusing from the capillary lumen following intravenous injection.

Following microinjection, it is possible that the pulse of radioactivity available to the enamel organ may be longer than that achieved intravenously due to the continued diffusion of ^{3}H-proline from the connective tissue into the enamel organ. Labeled amino acids are essentially cleared from the blood plasma by 1 hour after intravenous injection (Nakagami et al., 1971). Weinstock and Leblond (1974) found that the amount of free labeled proline in the blood plasma dropped sharply during the first 10 minutes after injection and concluded that a pulse of high radioactivity was achieved. However, a low but significant level of radioactivity persisted between 30 minutes and 30 hours after injection. In bone and dentin, some of the secreted proteins become part of a collagenous matrix which is transformed into mineralized products of the cells (Carneiro and Leblond, 1959; Young and Greulich, 1963; Weinstock and Leblond, 1974). Because of the appositional formation of dentin by odontoblasts, it becomes a continuous and stable record of the availability of labeled amino acids for incorporation into protein (Josephsen and Warshawsky, 1982). Although this study does not quantitate the amount of radioactivity available to the enamel organ following the initial pulse introduced by the microinjection, it does show that concurrent with the diffusion of ^{3}H-proline into

the enamel organ, there exists a similar rapid diffusion of ^{3}H-proline into the bloodstream. This was seen as a reaction band in the predentin as early as 30 minutes after microinjection. Figure 83 shows a reaction band in the predentin of the left hemi-mandible 4 hours after microinjection of the contralateral right hemi-mandible. Therefore, following microinjection of minute quantities (~10μCi) of ^{3}H-proline into a 100gm animal, the labeled amino acid rapidly diffuses into the local vasculature, is removed from this site by the circulation, and is incorporated into dentin of the contralateral incisor as a secretory product of the odontoblasts.

Several studies have investigated the permeability of the enamel organ and the enamel matrix to relatively large macromolcules such as serum albumin (Kinoshita, 1979; Ogura and Kinoshita, 1983; Okamura, 1983). In these studies, both endogenous and exogenous serum albumin were localized using the direct fluorescent antibody technique and radioautography. In the enamel maturation zone of the rabbit (Okamura, 1983), marked fluorescent staining of endogenous albumin was seen in the cytoplasm of ameloblasts and in the intercellular spaces between them. This staining was observed in both ruffle- and smooth-ended ameloblasts. The localization of intravenously injected, exogenous bovine serum albumin in the enamel maturation zone was identical to that of endogenous serum albumin. In no case was endogenous or exogenous serum albumin localized to the enamel matrix.

The finding that serum albumin was present in the intercellular space between ameloblasts is in agreement with observations of electron microscopic experiments using exogenous materials as tracers (Kallenbach, 1980a, 1980b; Skobe and Garant, 1974; Takano and Crenshaw, 1979). Ultrastructural investigations with or without exogenous tracers have indicated that

pinocytosis occurs in ameloblasts (Kallenbach, 1980b; Skobe and Garant, 1974; Josephsen and Fejerskov, 1977). It has been suggested that the movement of endogenous serum albumin in the ameloblast layer is similar to that of injected exogenous tracers (Okamura, 1983).

Salmon calcitonin has a molecular weight of approximately 3600D and was used in this study as a molecular weight marker to investigate the permeability of the enamel organ and enamel matrix. The present study has shown radioautographically that exogenous, ^{125}I-labeled salmon calcitonin, administered by the microinjection technique over the enamel maturation zone of the rat incisor, passes through the enamel organ and into the enamel matrix as soon as 10 minutes after microinjection. Furthermore, the label appears over the entire thickness of the enamel up to the dentino-enamel junction. This short time interval (10 min.) would suggest that the molecule is not a secretory product of the ameloblast and diffuses either extracellularly or transcellularly through the enamel organ to reach the enamel. Such a pathway suggests that either the proximal and distal junctional complexes of the ameloblast layer do not preclude the passage of ^{125}I-salmon calcitonin, or the putative transcellular transport is very rapid.

The results presented here are in agreement with those of Okamura (1983) in which relatively large exogenous molecules may reach and enter the ameloblast layer of the enamel maturation zone. Additionally, this study presents evidence that the enamel matrix is completely permeable to a molcule having a molecular weight of approximately 3600D. Microinjection experiments are presently underway using various molecular weight markers and using intravenous injections of the same molecules to serve as controls.

In conclusion, this study has demonstrated the feasibility of a drilling procedure that penetrates into the periodontal space overlying the

enamel organ. Furthermore, this procedure suggests that surgical penetration of the alveolar bone may cause trauma to the enamel organ and enamel. This study has also demonstrated the feasibility and advantages of a microinjection technique for in vivo experimentation on the enamel organ and enamel of the rat incisor.

TABLES

TABLE I

The relative percentages of the labial periodontal and dental compartments to the total area

Experimental animal	Window[1]	Compartments					
		Total	Alveolar bone	Periodontal space	Enamel organ	Enamel	Venous sinuses
1	a	100	42.7	27.8	23.9	6.9	0.3
	b	100	43.4	25.1	24.0	8.7	4.8
	c	100	42.9	23.0	24.3	10.5	5.2
2	a	100	51.5	26.3	18.8	5.4	13.7
	b	100	47.4	25.1	20.4	6.8	4.4
	c	100	42.1	25.9	23.0	8.8	3.7
3	a	100	43.3	26.0	22.4	8.5	4.6
	b	100	39.7	26.4	24.1	10.1	5.0
	c	100	38.9	25.7	24.9	12.5	9.3
4	a	100	43.2	29.8	20.3	5.6	10.7
	b	100	39.6	29.1	23.3	8.5	10.2
	c	100	35.3	29.0	24.0	11.1	8.8
5	a	100	49.7	25.6	18.4	4.9	7.3
	b	100	47.6	24.5	20.3	7.3	6.8
	c	100	43.9	25.2	21.1	8.7	9.4
AVG.		100	43.4	26.3	22.2	8.3	6.9

[1]The rectangular viewing limits used to measure the compartments

TABLE II

The relative percentages of the labial periodontal and dental compartments to the total thickness

Experimental animal	Window[1]	Compartment				
		Total	Alveolar bone	Periodontal space	Enamel organ	Enamel
1	a	100	43.4	28.9	21.9	5.9
	b	100	45.9	24.1	22.4	8.0
	c	100	41.9	23.9	22.8	9.7
2	a	100	45.4	31.7	18.7	4.9
	b	100	49.7	25.1	20.0	6.2
	c	100	41.7	27.2	22.6	8.3
3	a	100	45.8	25.8	21.6	6.7
	b	100	38.5	28.5	23.5	9.3
	c	100	39.9	24.5	24.0	11.5
4	a	100	43.4	30.8	20.6	5.2
	b	100	44.2	26.0	23.3	6.9
	c	100	39.0	29.1	22.3	9.7
5	a	100	53.4	24.9	17.0	4.4
	b	100	50.9	23.4	19.5	6.4
	c	100	48.5	23.9	21.3	7.9
AVG.		100	44.8	26.5	21.4	7.4

[1]The rectangular viewing limits used to measure the compartments

FIGURES AND LEGENDS

Figure 1

Enlargement of the right hemi-mandible of a Sherman strain rat sacrificed 24 d after drilling. The drill used for the surgery is shown above the hole in the alveolar bone (black arrow). The alveolar bone may be drilled anywhere along its inferior border where it overlies the secretion or maturation zones of the incisor. Note the bone remodeling surrounding the hole. The enamel has moved away from the hole due to the continuous eruption of the tooth and appears as a shallow, white pit in the erupted enamel (white arrow). X 6.5


1

Figure 2

Dental burs of different size, shape and blade configuration used to penetrate the alveolar bone. X 20

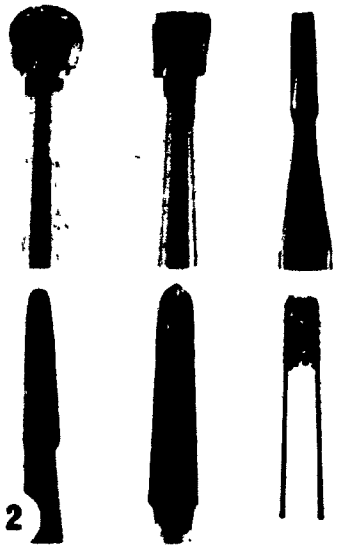
2

Figure 3

The microinjection apparatus showing the column stand (A) on which was mounted a micromanipulator (B). A micrometer (C) was inserted into the clamping mechanism (D) of the micromanipulator and a 100 µl microsyringe with a 33 guage luer lock needle (E) was fitted to the micrometer. This assembly allows for the fine vertical and horizontal movements necessary for microinjections. X 0.85

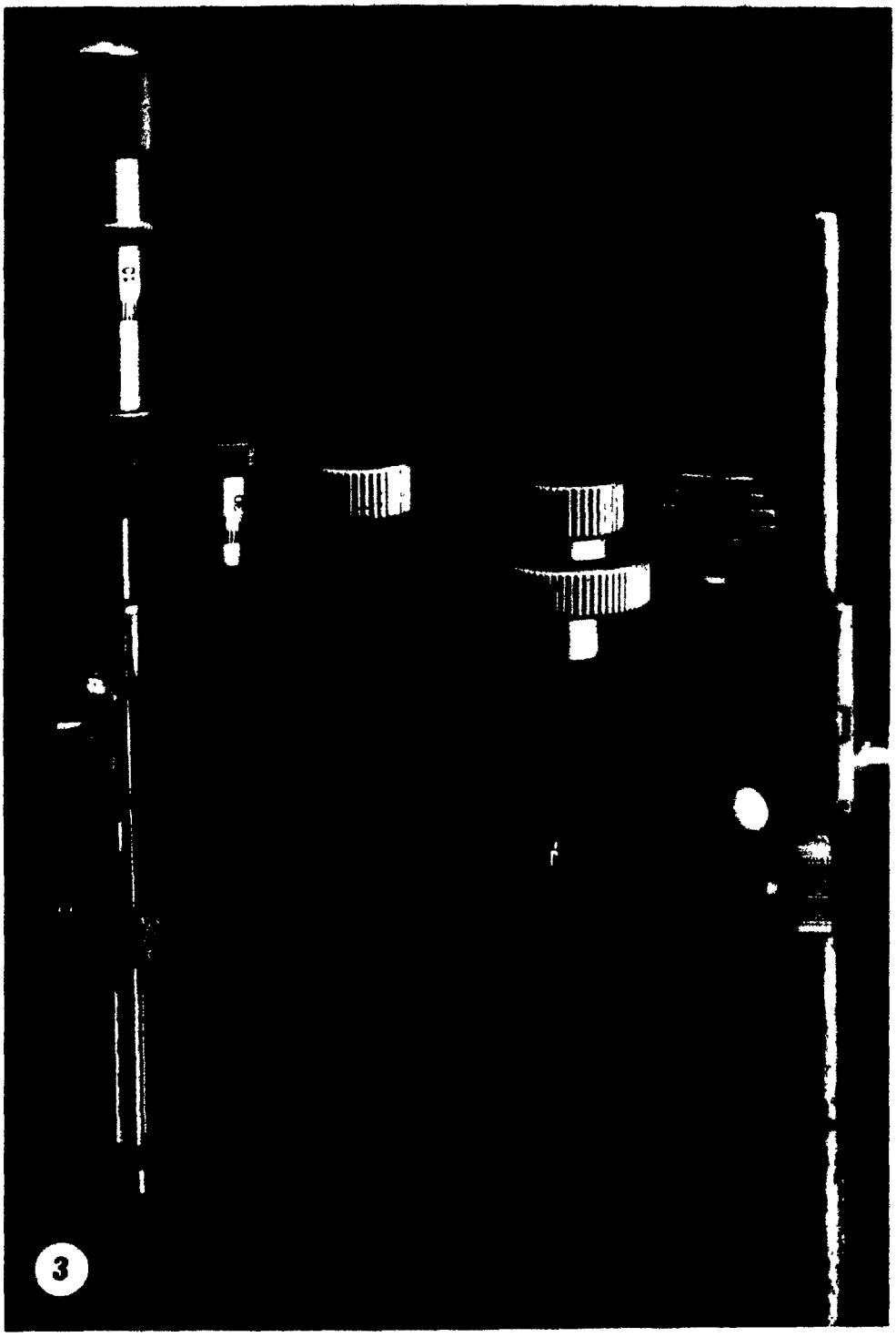
3

Figure 3.1

Photomicrograph of the inner enamel secretion zone of the rat incisor corresponding approximately to the area where the alveolar bone was drilled. Superimposed over the photomicrograph are the rectangular viewing limits (R) used to delineate the compartments from which the areas and thickness were measured using a MOP-3. The bar to the left of the rectangle illustrates how the thickness of each compartment was measured. Three such rectangular areas were measured in each animal. ab, alveolar bone compartment; vs, vascular sinus compartment; ps, periodontal space compartment; eo, enamel organ compartment; e, enamel compartment. The boundaries of each compartment are outlined in the text, page X 165


R
VS
DS
31

Figure 4

A longitudinal section of the right hemi-mandible showing the original drill site (B) in the alveolar bone (ab) and the trauma to the underlying dental tissues (E) that has moved incisally away from the drill site over 2 d (the large arrow indicates the direction of tooth eruption). "Healthy" ameloblasts are now found under the bone lesion. Note the vascularity of the region between the enamel organ and the alveolar bone, the periodontal space (PS). am, ameloblasts; en, enamel; d, dentin. X 130

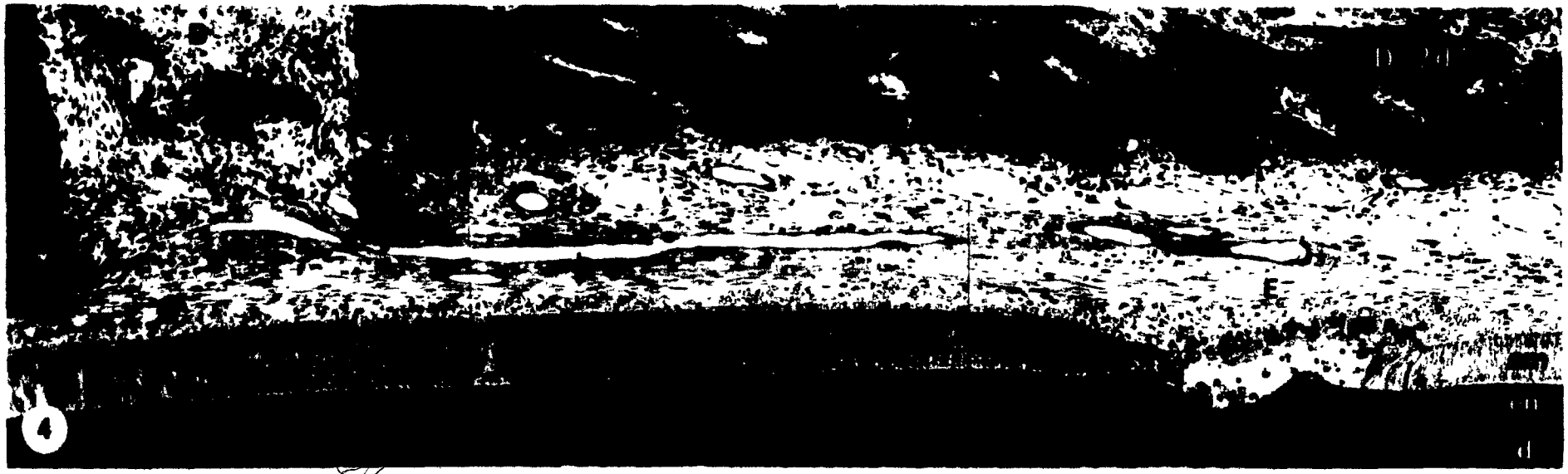
4

Figures 5,6

Bone lesions drilled over the enamel secretion zone in which the animals were sacrificed 2 d after drilling. Bone fragments (straight arrows) are seen at, or near the drill site, some of which may be surrounded by osteoclasts. Bleeding has occurred in the periodontal space (PS) and extends laterally from the drill site (curved arrow). Note the "healthy" enamel and enamel organ under the bone lesion. ab, alveolar bone; eo, enamel organ; e, enamel; c, vascular channel. X 250


2d
ab
e
5


2d
6

Figure 7

A bone lesion showing a bone flap (white arrow) caused by the drilling. The hemi-mandible was drilled over the enamel secretion zone. The black arrow indicates the direction of tooth eruption. ab, alveolar bone; am, ameloblasts. X 250

Figure 8

Higher magnification of the bone flap in Figure 7. The bone flap (bf) compresses the enamel organ as it "squeezes" underneath the flap during eruption. The integrity of the enamel organ is lost incisal to the bone flap. si, stratum intermedium; AM, ameloblasts. X 400


2d
7


8

Figures 9,10

Examples of bone lesions that did not cause trauma to the underlying enamel (e) or enamel organ (eo). Complete penetration of the alveolar bone was achieved and the animals were sacrificed immediately. The drill entered a vascular sinus (vs) but there was no rupture of the endothelium on the side facing the enamel organ (between the arrows). b, red blood cells; d, dentin. X 140


VS
9


Oh
b
VS
e
d
10

Figures 11,12

Electron micrographs showing bone fragments (b) lined with active osteoclasts. These osteoclasts are multinucleated, contain numerous mitochondria (m), and show the characteristic clear (cz) and ruffled zones (rz) suggestive of bone resorption. Fig. 11, X 7,000; Fig. 12, X 12,250

Figure 13

Electron micrograph of an osteoblast-like cell found within the connective tissue plug of the bone lesion. Note the numerous and distended rough endoplasmic reticulum, frequent mitochondria, and the numerous collagen fibrils (cf) seen at the cell surface (arrows). X 10,500

Figure 14

Electron micrograph of an osteoblast (ob) frequently found lining the cut edges of the bone lesion. pb, prebone; b, bone. X 14,000


11


12

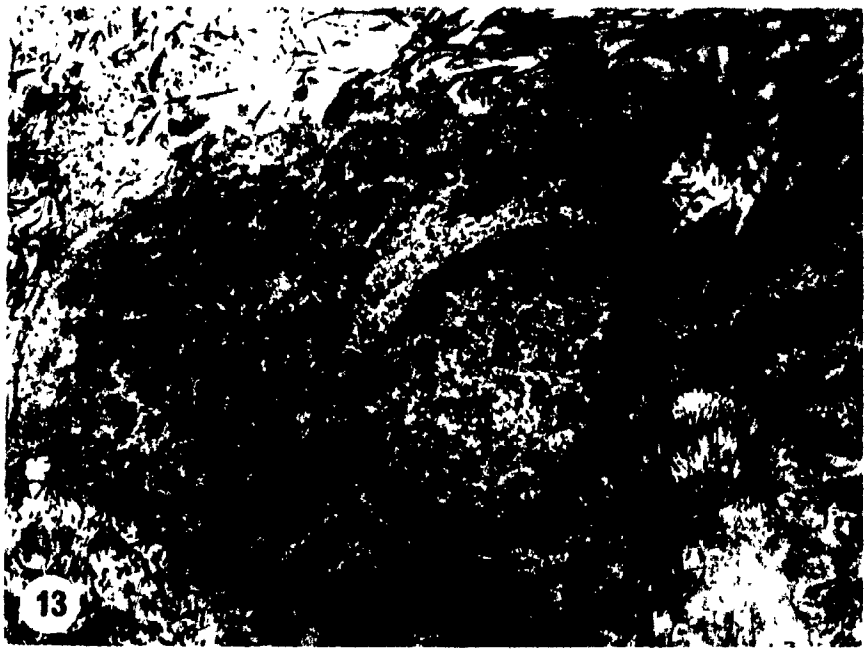
13

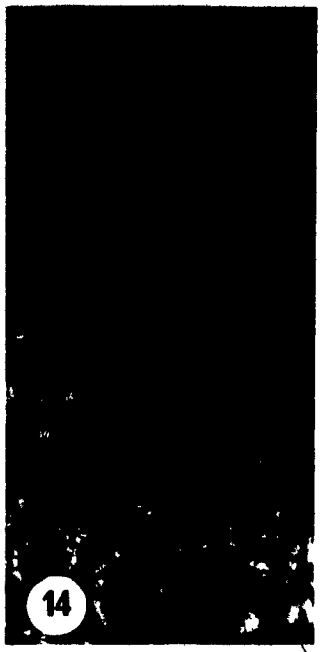
14

Figures 15,16

Enamel lesions in which the animals were sacrificed immediately after drilling (0 h). The enamel organ (eo) and enamel (e) have been completely stripped from the dentin (d) and the enamel organ displays a "gushing" effect. Bone fragments (bf) and enamel fragments (large arrow) may be seen at the site of the lesion. In most cases, the dentino-enamel junction (DEJ) shows no sign of trauma (between arrows in Fig. 16). si, stratum intermedium; am, ameloblasts. X 220

Figures 17-19

Enamel lesions at 0 h in which the enamel organ (eo) is intact for the extent of the lesion. Again the enamel (e) is completely removed from the dentin (d) and the dentino-enamel junction (DEJ) has remained unscarred (arrows). The enamel that remains in the lesion is fragmented. Serial sections through these lesions show the enamel organ to be ruptured at some point over the enamel lesion. PS, periodontal space; pl, papillary layer; si, stratum intermedium; am, ameloblasts. X 220


PS
17

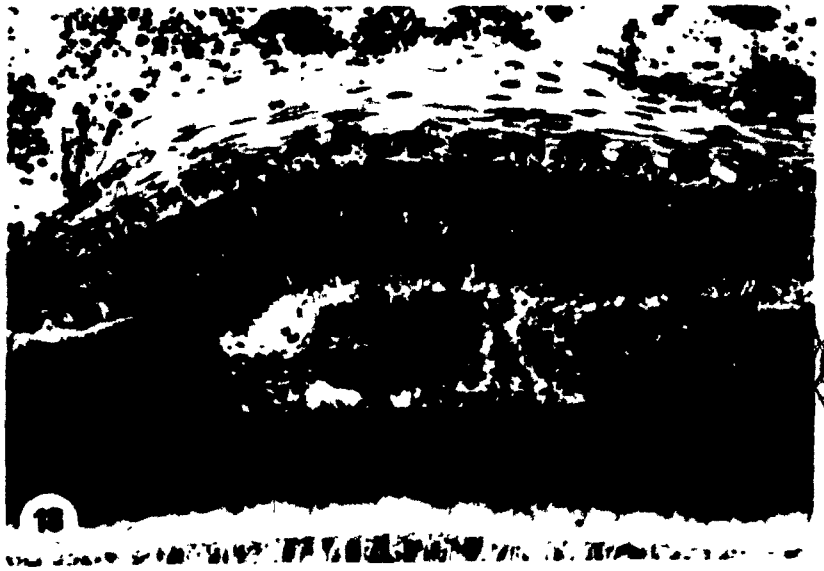
18


19

Figures 20,21

Lesions at 12 h after drilling. Remnants of enamel (en) remain at the dentino-enamel junction (DEJ) and many red blood cells (rbc) are present at the site of the lesion. Ameloblasts (am) have been torn away from the enamel, their nuclei are pyknotic, and they show signs of degeneration. Rod profiles appear separated (arrow). PS, periodontal space; si, stratum intermedium. X 325

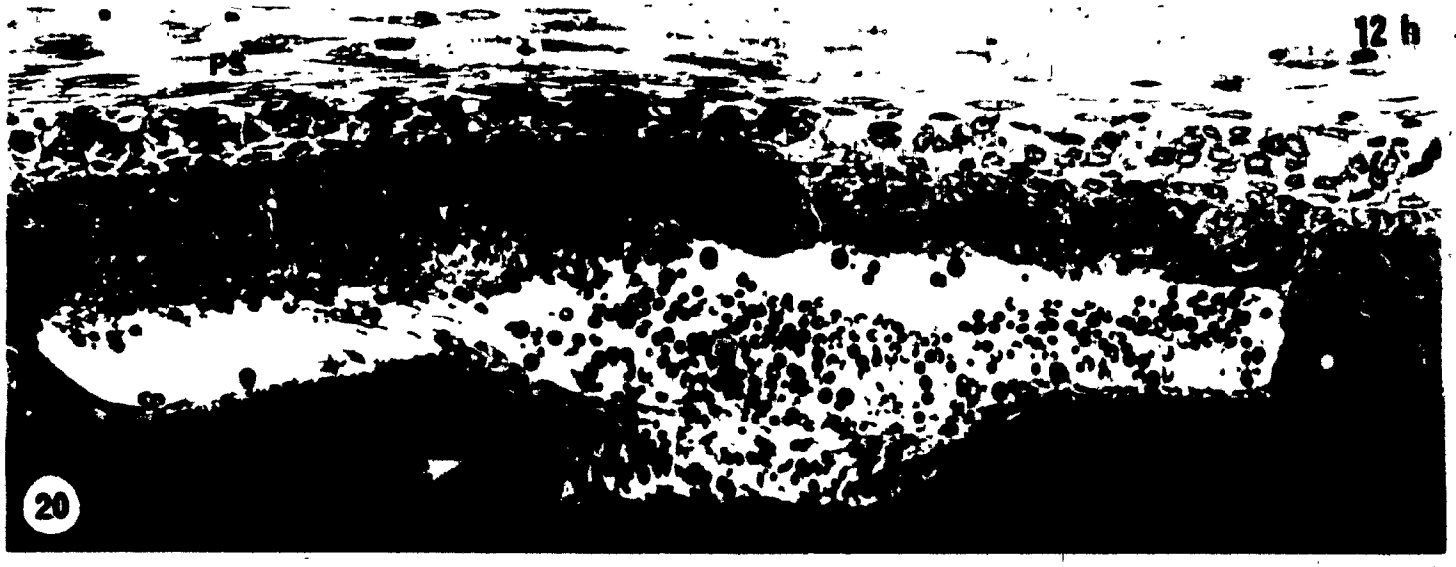
PS
12 h
20

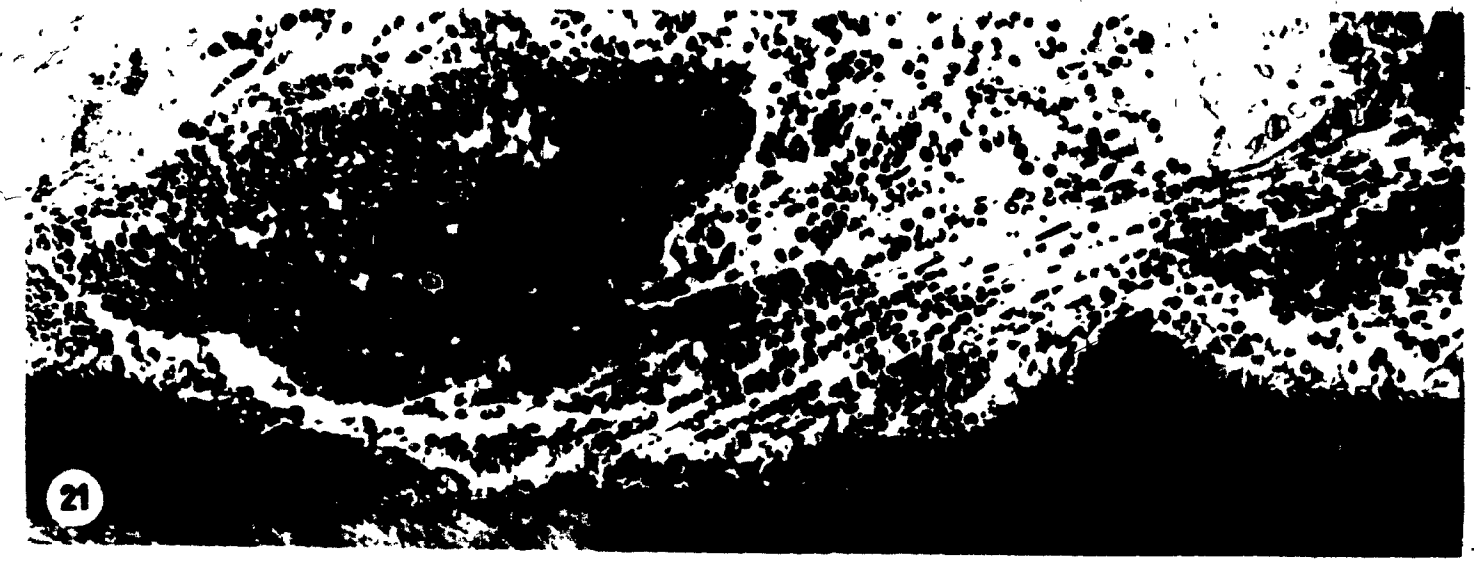
21

Figures 22,23

Lesions at 2 d after drilling. The enamel (en) is completely removed at the dentino-enamel junction (DEJ). The DEJ is unscarred and pools of blood (arrows) are seen at the lesion site. Note that the vasculature of the periodontal space (PS) remains relatively intact. d, dentin; ab, alveolar bone. X 120


3d
ps
en
DEJ
d
22

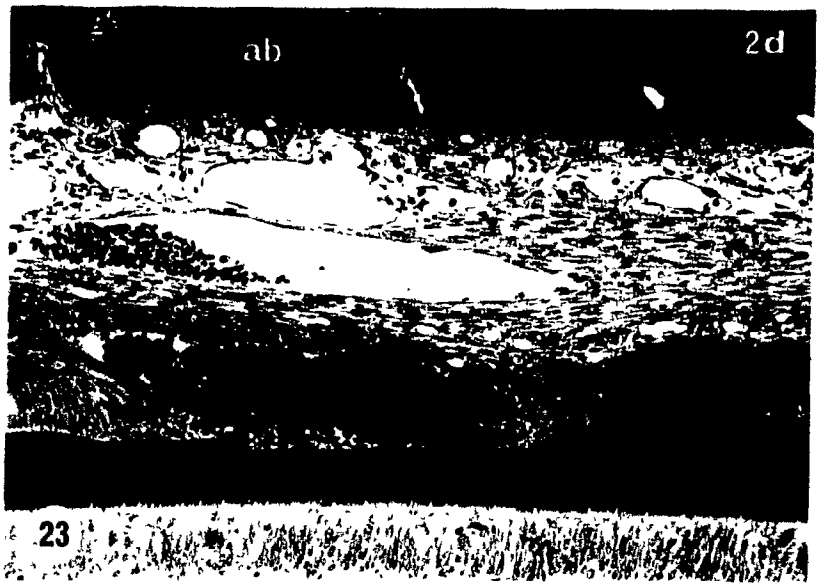
ab
2d
23

Figure 24

Lesion at 2 d after drilling. This lesion shows a typical pool of blood (rbc), a ruptured enamel organ and a lack of enamel at the lesion site. At the dentino-enamel junction, extending the width of the lesion, is a thin layer of dark-staining material (white arrow). Between ameloblasts (am) at the periphery of the lesion are accumulations of an amorphous dense material (black arrow). Note cells (c) apposed to the ragged edges of the enamel. en, enamel; d, dentin. X 400.

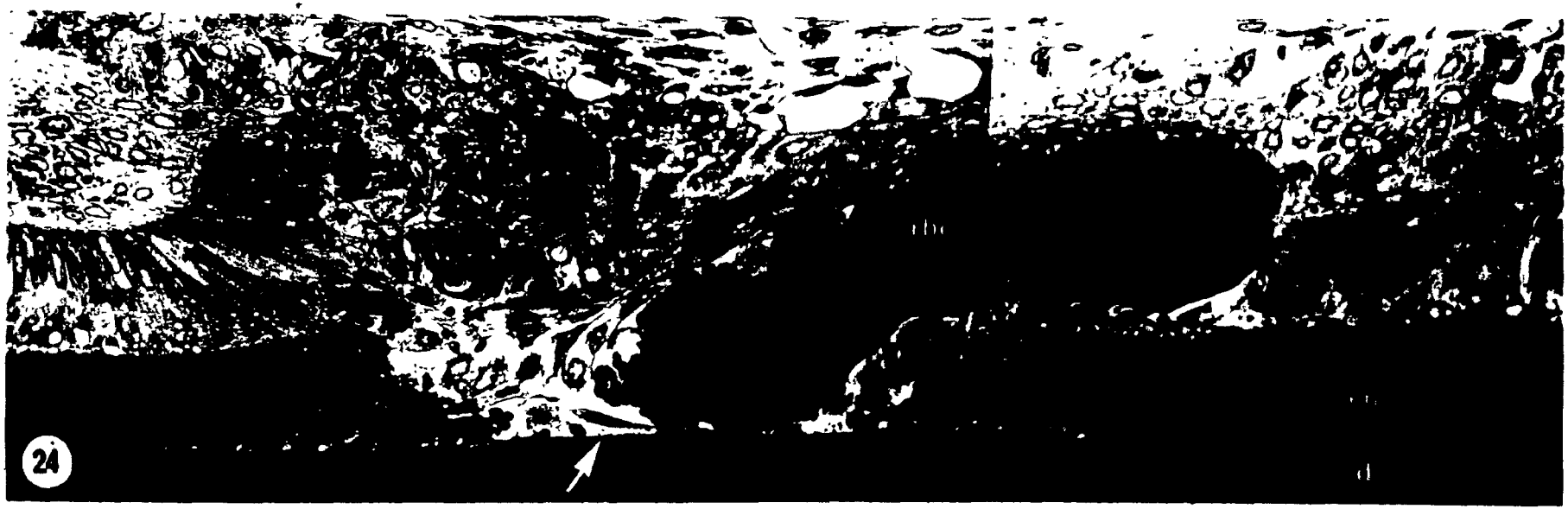
24

Figures 25,26

Lesion at 2 d after drilling. The drilling occurred in the outer enamel secretion zone and the enamel lesion has since moved into the enamel maturation zone (MAT). The capillary network (c) of the papillary layer may be followed over the lesion. Smooth-ended ameloblasts (curved arrow) of the maturation zone extend over the ragged edge of the enamel (en). These cells still show intimate contact with the enamel. Separated rod profiles are apparent (white arrow). Cells may be seen to "creep" between the enamel and the dentin at the dentino-enamel junction (black arrow). Fig. 25, X 120; Fig. 26, X 400

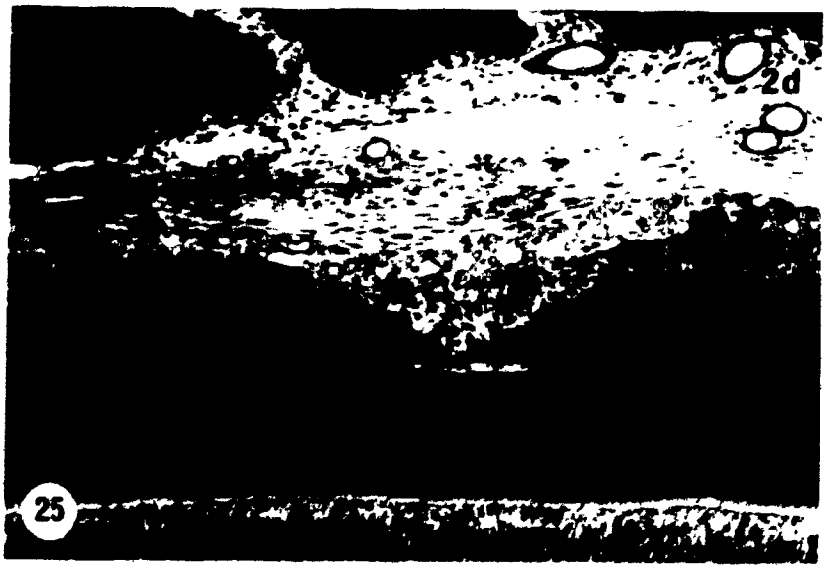
2d
25


C
en
26

Figures 27,28

Lesion at 2 d after drilling. Cells appearing to belong to the enamel organ seem to continue across the lesion. The dark-staining material (white arrow) is seen at the dentino-enamel junction. The enamel depth is constant for part of the lesion (s) and may be due to an inhibition of secretion in this area. Accumulations of red blood cells, singly stacked or packed in oval clusters not bound by endothelium, are found between ameloblasts (black arrows). vs, vascular sinus; si, stratum intermedium; am, ameloblasts; d, dentin; c, capillary; PS, periodontal space. Fig. 27, X 120; Fig. 28, X 400


2d
VS
27


2d
PS
C
C
S
28
d

Figure 29

Lesion at 2 d after drilling in which the plane of section passes through the periphery of the lesion. Serial sections show the enamel to be completely removed at the center of the lesion. The ameloblasts (am) have decreased in height and the enamel (en) in this area maintains a constant thickness (arrowheads). Accumulations of red blood cells (arrows) are found between ameloblasts. d, dentin. X 400


29

Figures 30,31

Lesions at 5 d after drilling. The lesions are similar to those in animals sacrificed at other time intervals. The enamel (en) is completely removed and there is a dark-staining layer (arrow) at the dentino-enamel junction. The enamel organs are ruptured and cells of unknown origin are located in the lesion. am, ameloblasts; d, dentin; ps, periodontal space. X 325

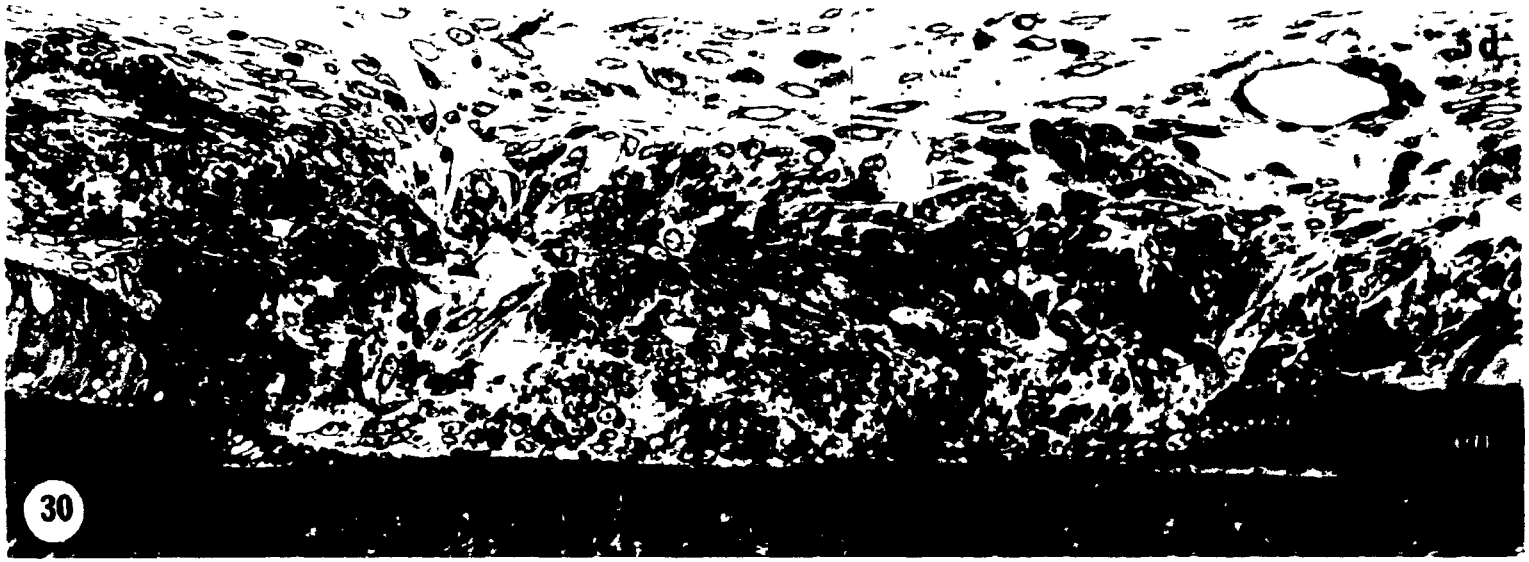
30

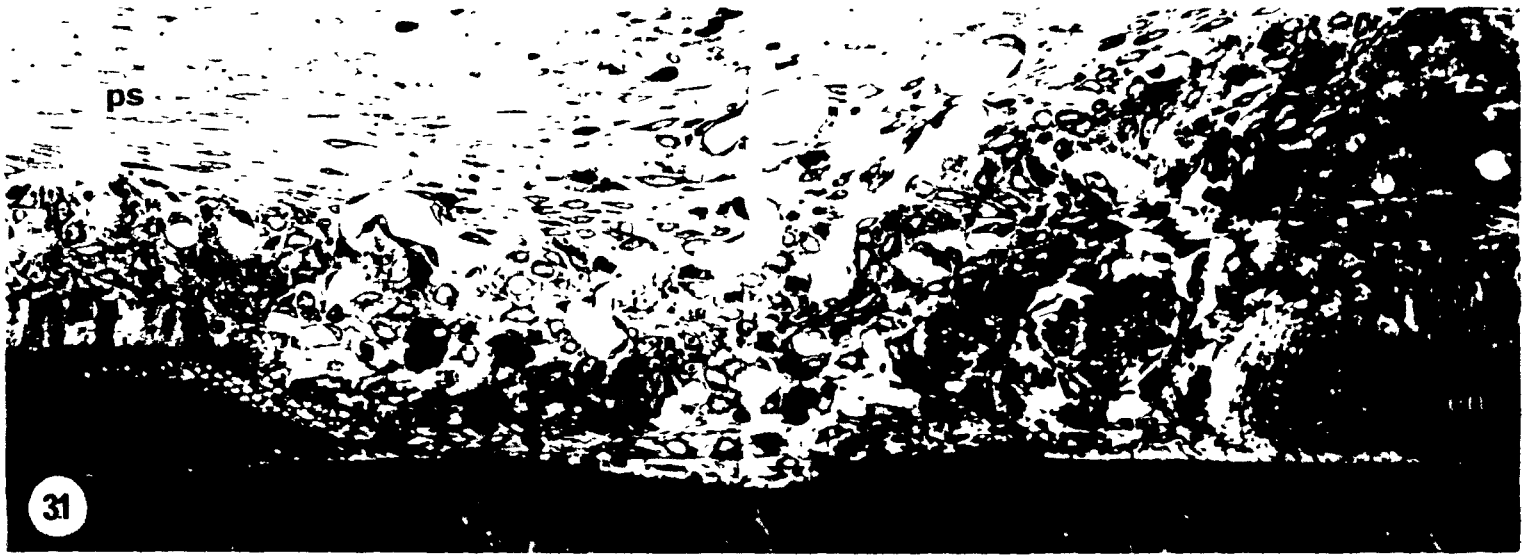
ps
31

Figures 32,33

The infranuclear zone (IZ) of secretory ameloblasts showing the presence of red blood cells (arrows) located interstitially between ameloblasts (am). M, mitochondria. Fig. 32, X 6,000; Fig. 33, X 7,500

Figure 34

Electron micrograph showing red blood cells (arrow) in the periodontal space (PS) caused by trauma to the vasculature during drilling. CF, collagen fibrils. X 10,500

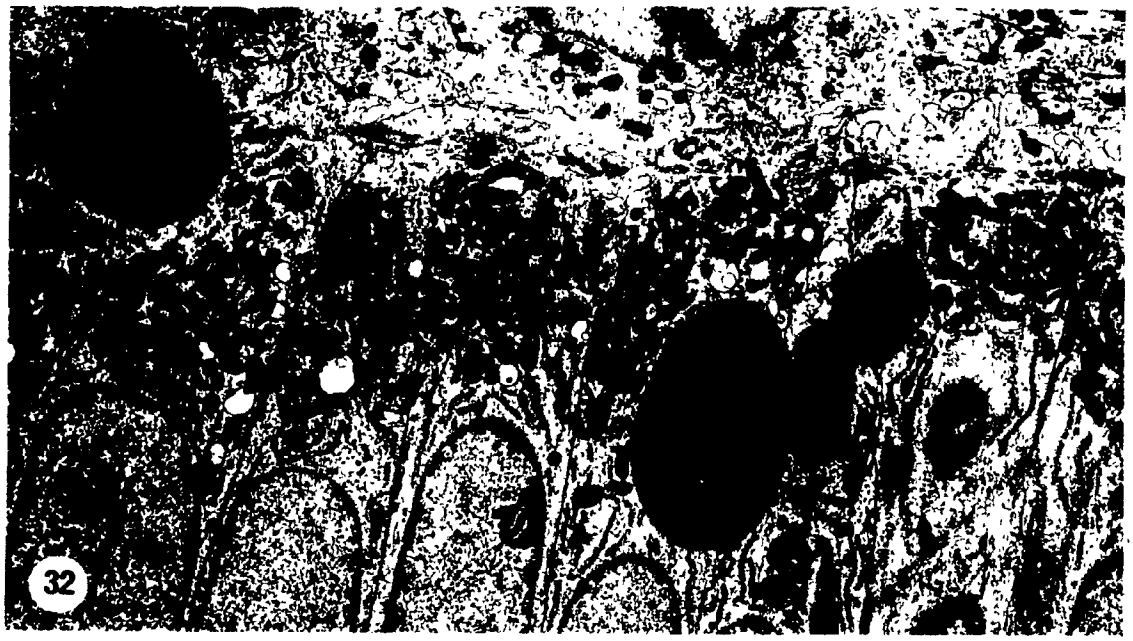
32

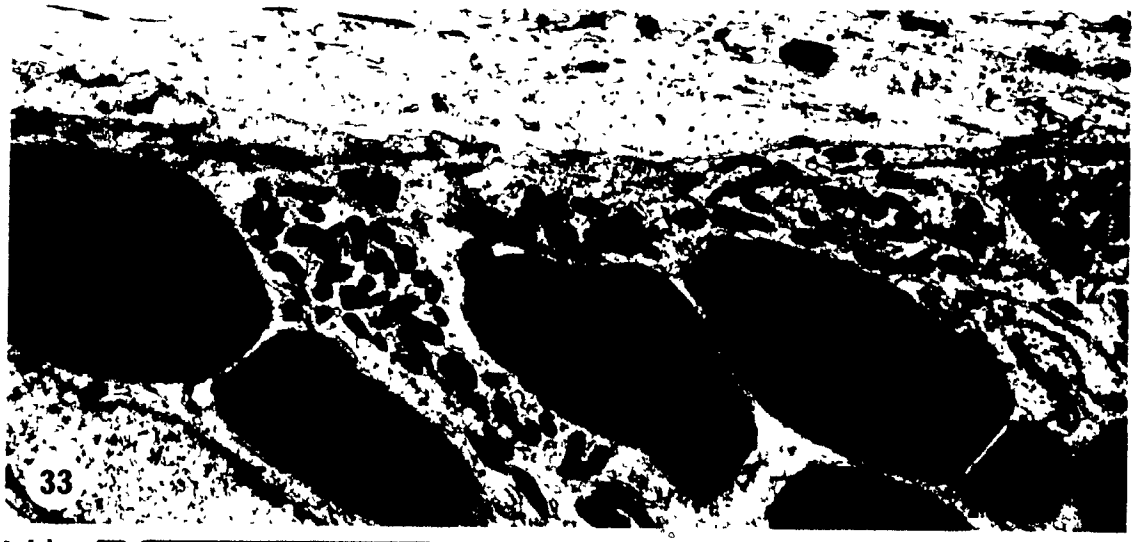
33


34

Figures 35-37

Electron micrographs showing mononuclear cells with mitochondria and moderate amounts of rER apposed to the irregular surface of the enamel (en). The cell membranes follow the contour of the enamel and laterally make junctional contacts (j) with each other. The enamel appears mottled and may contain a lighter-staining, granular substance (g). Observed between cells is an amorphous, homogeneous, light-staining material (asterisk) within which may be found accumulations of a darker-staining material (arrows). Fig. 35, X 7,000; Fig. 36, X 28,000; Fig. 37, X 14,000


en
g
35

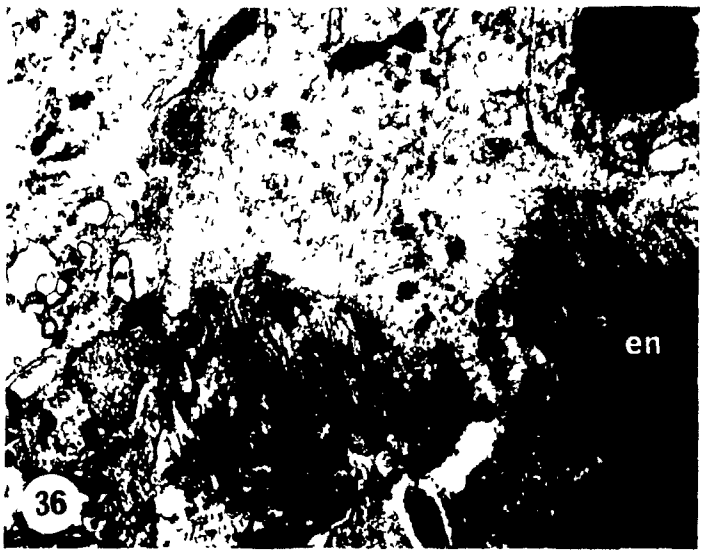
en
36


en
37

Figures 38-41

Higher magnification of the dark-staining material between cells lining the enamel. This material may be of a granular and irregularly clumped nature (G) or homogeneously dense (H). The lighter-staining material between cells (asterisk) is not always present but the cells frequently show finger-like projections into the intercellular space (arrows). Fig. 38, X 49,000; Fig. 39, X 24,500; Fig. 40, X 38,500; Fig. 41, X 38,500

38
39
40
41

Figures 42-44

Osteoclast-like cells apposed to enamel (en) at the periphery of the lesion. They possess clear zones (CZ) and numerous mitochondria (m) characteristic of osteoclasts. Seen within the clear zone are membrane-bound structures containing what appears to be enamel (arrows). They have finger-like projections (f) into the extracellular space away from the enamel, but otherwise the cell membrane follows the irregular surface of the enamel. d, lipid droplets. Fig. 42, X 14,000; Fig. 43, X 19,250; Fig 44, X 31,500


42


43


44

Figure 45

Electron micrograph of a cell apposed to the irregular surface of enamel (en) at the periphery of the lesion. Cytoplasmic extensions (ce) are seen to interdigitate with the enamel. Mitochondria (m) are numerous and heterolysosomes (ly) may be seen. X 10,500

Figure 46

Electron micrograph of a cell apposed to the enamel (en) in which a ruffled border is present (RB). Dark-staining material (arrow) may be found within the ruffled border. A grainy precipitate (p) is seen in the extracellular space of the ruffled border and in the adjacent enamel. m, mitochondria. X 17,500

Figure 47

Electron micrograph showing interdigitation of the cytoplasmic extensions (ce) and enamel (en). Vacuoles (v) are present, some of which are continuous with the cell membrane (arrow) and show possible uptake of a dark, amorphous material. Well-developed desmosomes (d) can be seen. X 31,500


45


46


d
d
v
47

Figure 48

Higher magnification of the cell membrane-enamel junction showing numerous mitochondria (m). en, enamel. X 35,000

Figures 49,50

Electron micrographs showing membrane-enamel relationships. Vacuolar (v, Fig. 49) and vesicular (vs, Fig. 50) structures are numerous and, occasionally vesicles or coated pits are continuous with the cell membrane (arrowheads) and are therefore open to the enamel (en). The vesicular structures may be filled with material similar in nature to enamel (Fig. 50). Membrane-bound granules, similar to secretion granules of ameloblasts, are sometimes observed (arrows). m, mitochondria. Fig. 49, X 17,500; Fig. 50, X 42,000

48
49
V
50

Figures 51-54

Different appearances of enamel at the periphery of the lesion. Rod (R) and interrod (IR) profiles appear separated and frequently a lightly granular (g) or filamentous (f) material is dispersed between the rod and interrod enamel. Occasionally, a dense sheath delineates the rod profiles (arrow, Fig. 53). Fig. 51, X 7,000; Figs. 52,53, X 14,000. Fig. 54, X 31,500

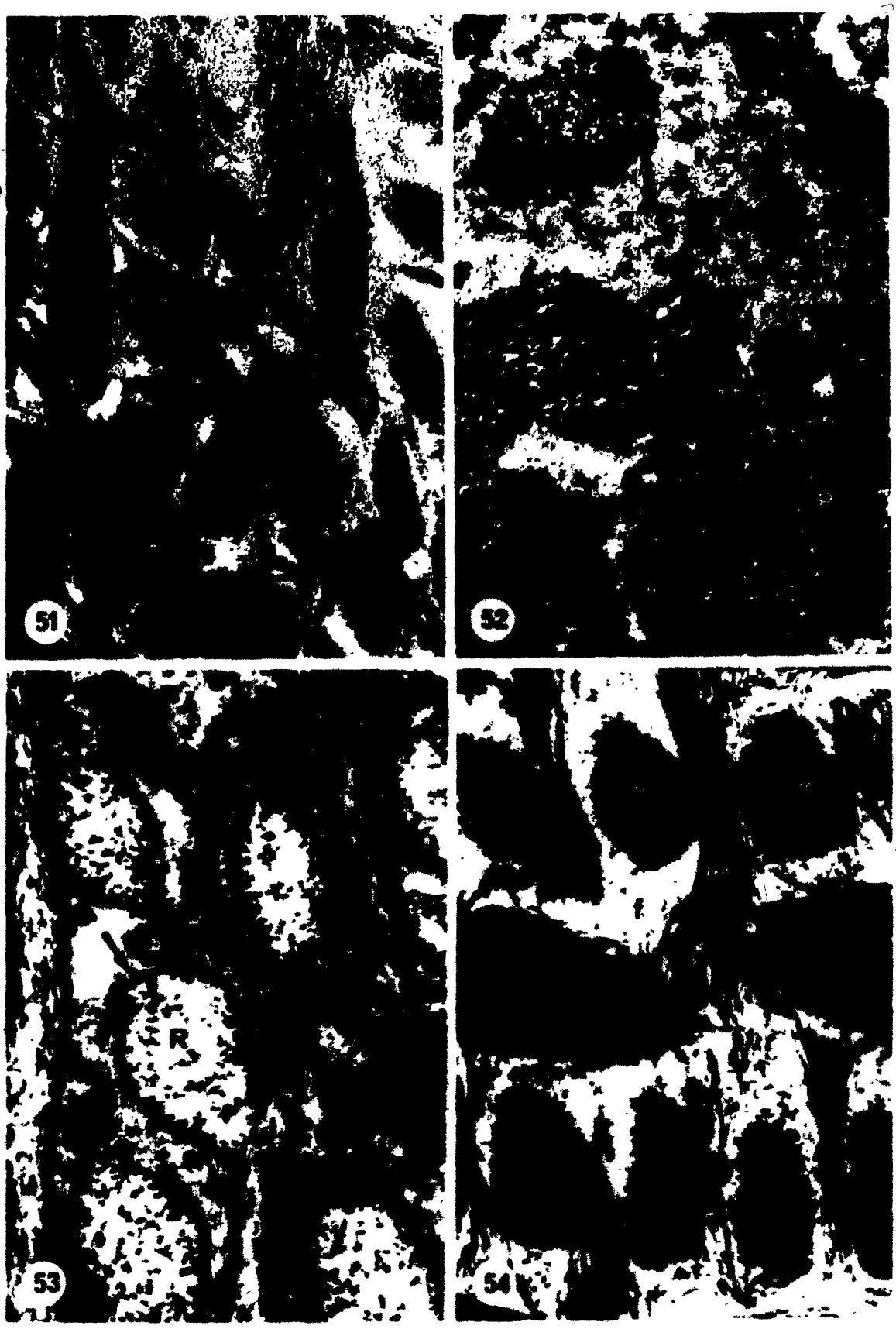
51
52
R
53
54

Figures 55,56

Association of amorphous, dense globules (g) with enamel (en) at the periphery of the lesion. These globules are most frequently seen at the rod-interrod interface; are irregular in shape, and are not membrane-bound. Fig. 55, X 31,500. Fig. 56, X 42,000

Figure 57

Electron micrograph of deeper enamel showing globules (g) at the rod (R)-interrod (IR) interface. X 24,500

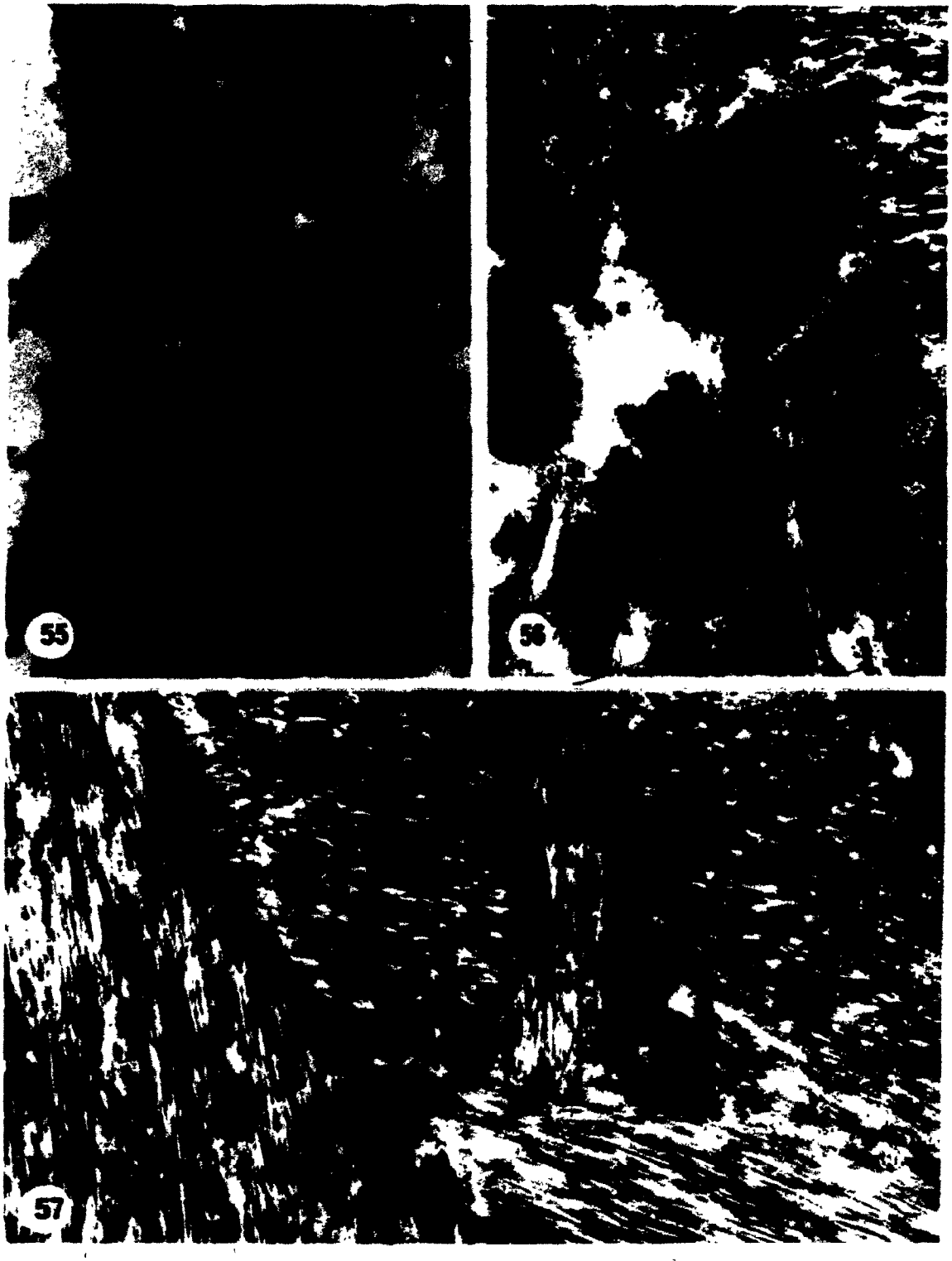
55
56
57

Figures 58-62

Dense, amorphous globules (g) seen in close association with membrane remnants (large arrows). Most frequently, the globules are aligned between membranes and enamel (en) but may sometimes be seen on the other side of the membrane or completely enclosed by membrane (Fig. 61). Figs. 58,59, X 28,000; Figs. 60,61, X 38,500; Fig. 62, X 66,500

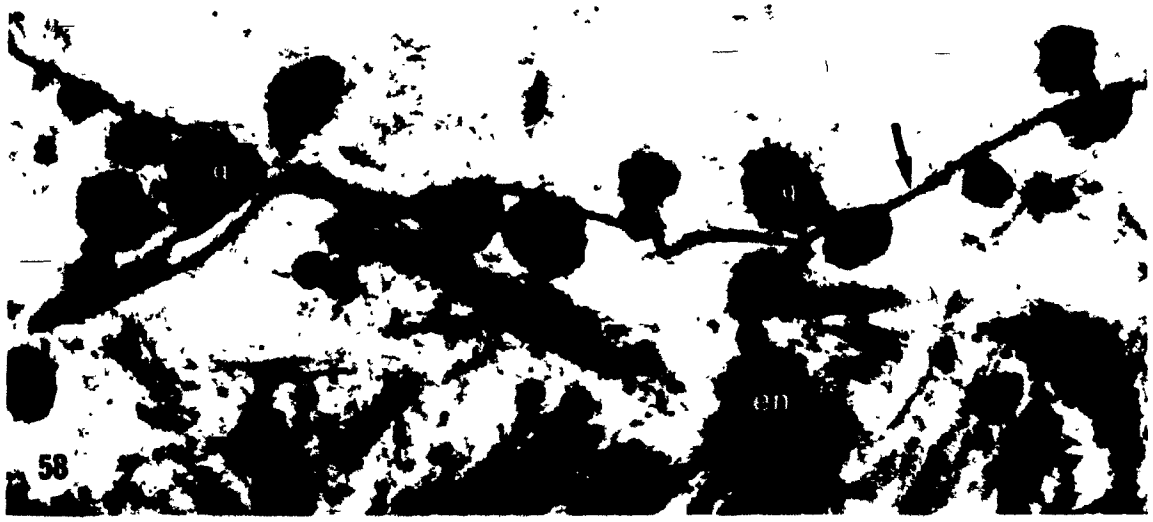
58


59


60


61


62

Figures 63,64

Amoeboid cells "crawling" through the separations of rod (R) and interrod (IR) enamel. These cells have a prominent Golgi apparatus (G), relatively little rER, and an abundance of lysosomes (ly). Fig. 63, X 8,000; Fig. 64, X 10,500

Figures 65,66

Similar cells as above but at the dentino-enamel junction. Cytoplasmic lipid droplets (Li) are frequently observed. en, enamel. Fig. 65, X 5,750; Fig. 66, X 14,000

63

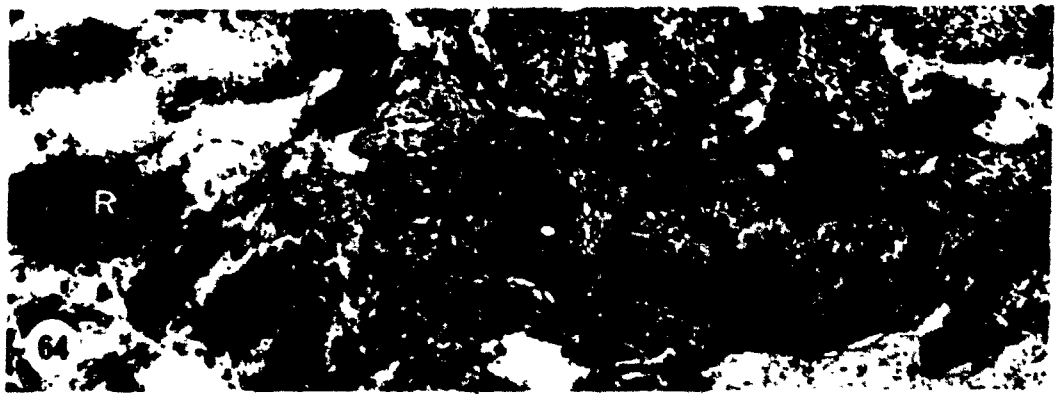

64

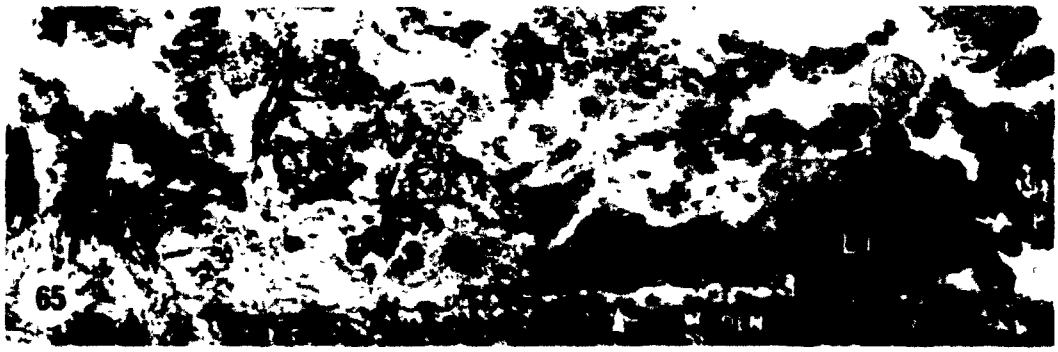

65

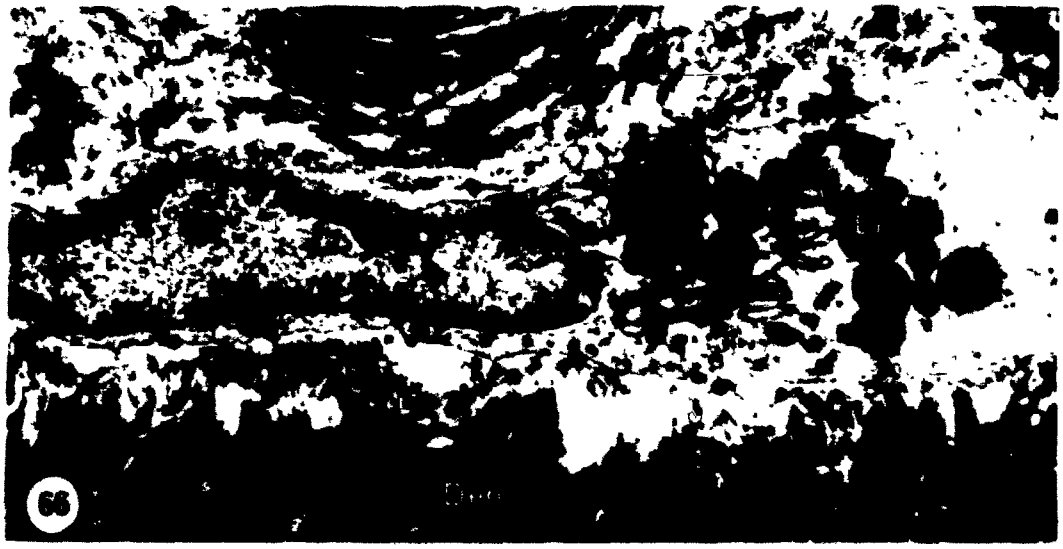

66

Figures 67-69

Electron micrographs at the center of the lesion. The enamel has been completely removed and an amorphous layer of material is seen at the dentino-enamel junction (arrows). This layer completely covers the dentin (Den), may vary in thickness, and extends to the periphery of the lesion where enamel again overlies the dentin. PMN, polymorphonuclear leucocyte. X 10,500

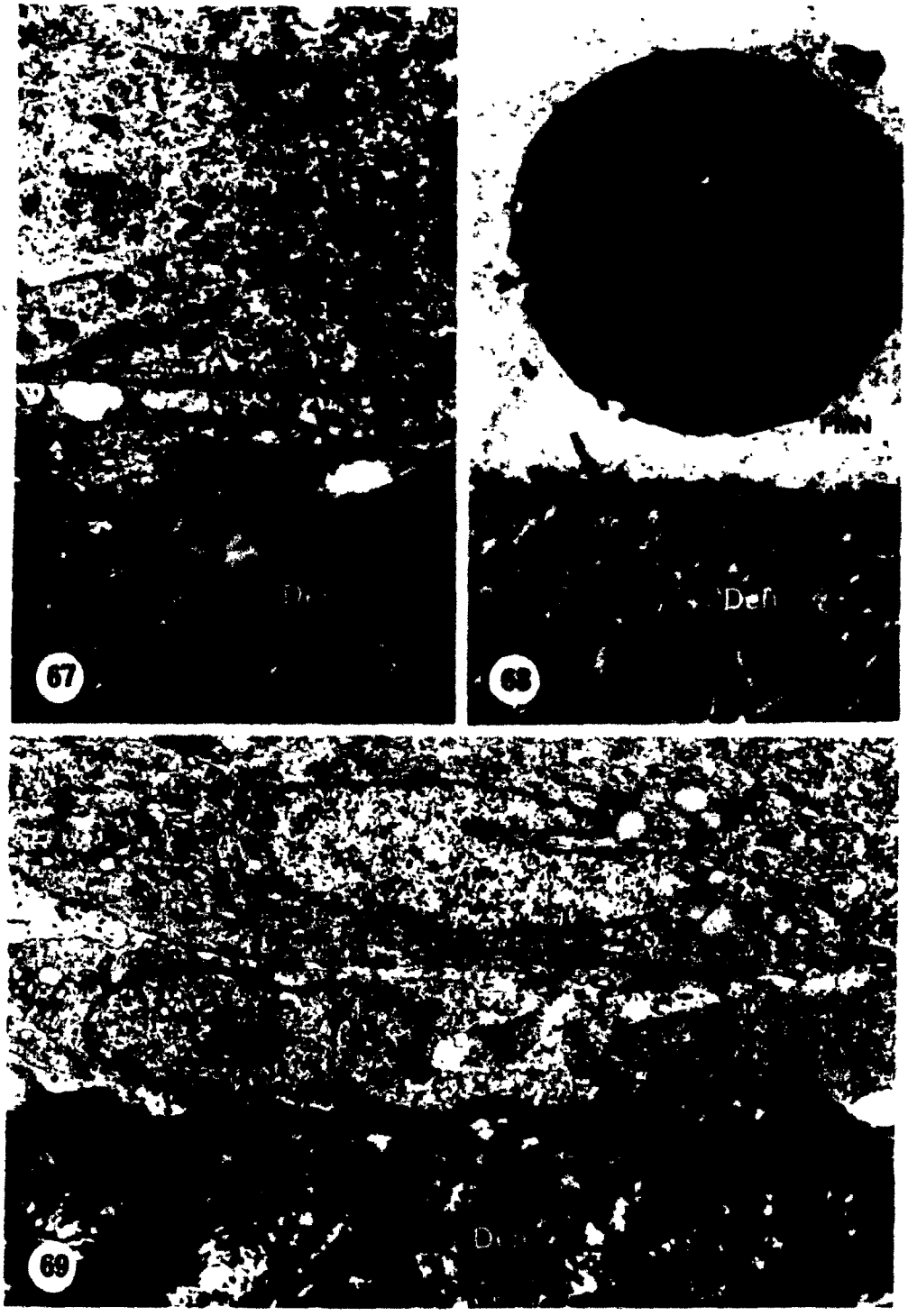
67
68
69

Figures 70-72

Higher magnification of the amorphous layer at the dentino-enamel junction (asterisks). This layer seems to be bounded by two zones of increased density (arrows). Den, dentin; Fig. 70, X 23,100; Fig. 71, X 42,900; Fig. 72, X 33,000

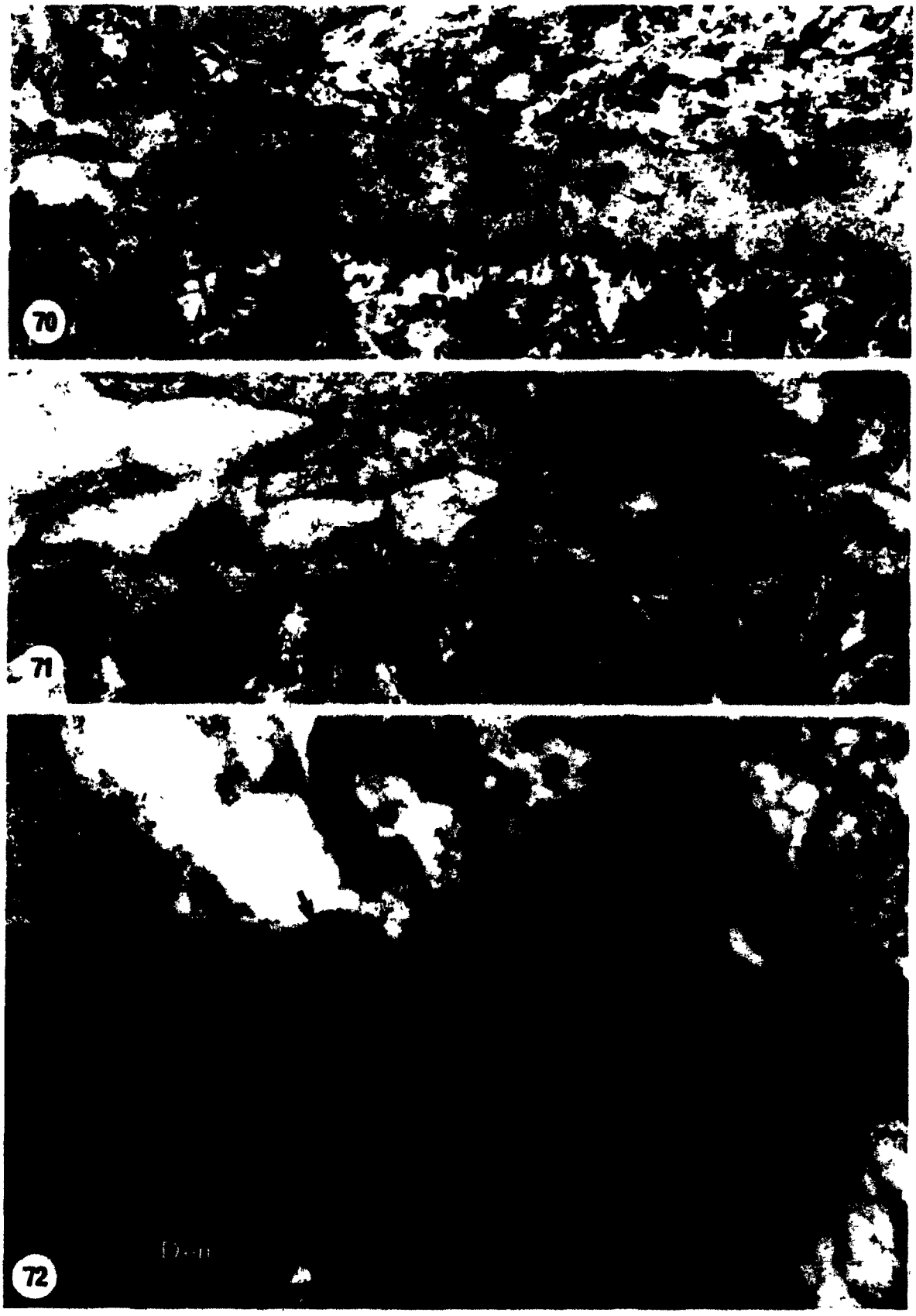
70
71
72

Figures 73,74

Photomicrographs of animals sacrificed immediately after a "red hot" bur was placed in a shallow pit drilled in the alveolar bone (ab). The hemi-mandibles were drilled over the secretion zone and the outline of the drill penetration into the alveolar bone is clearly visible (arrows). Note that the enamel organ (eo) and the enamel (e) are completely intact. Leucocytes and red blood cells are numerous at the drill site. vs, vascular sinus. X 140

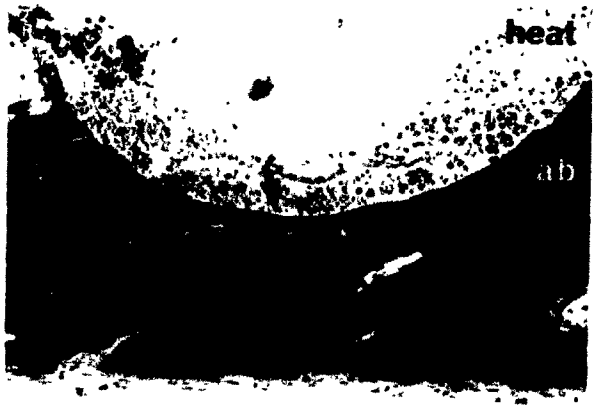

vs

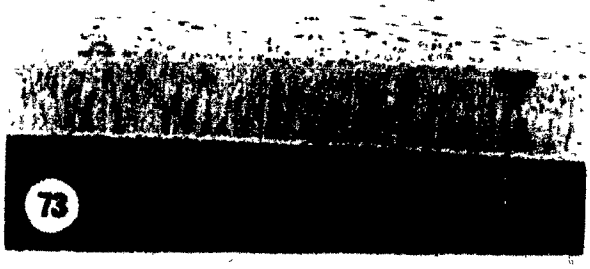

vs

Figures 75,76

Lesions in which burs of different size, shape and blade configuration were used to penetrate the alveolar bone. The animals were sacrificed immediately after drilling (0 h). The lesions were similar to those previously described at 0 h post-drilling in which the enamel organ (eo) is torn away from the enamel (e), the enamel is completely removed from the dentino-enamel junction, and the dentin (d) remains unscarred. rbc, red blood cells. X 140


75


76

Figure 77

Radioautographic localization of ^{3}H-proline 10 minutes after microinjection. The reaction is over the supranuclear zone of the secretory ameloblasts (AM). EN, enamel. X 800

Figure 78

Radioautographic localization of ^{3}H-proline 30 minutes after microinjection. The reaction is seen over Tomes' processes as well as the supranuclear zone of the ameloblasts. X 800

Figure 79

Radioautographic localization of ^{3}H-proline 1 hour after microinjection. A heavy reaction band is seen over Tomes' processes and part of the enamel matrix. Grains are still seen over the supranuclear zone of the ameloblasts. X 600

Figure 80

Radioautographic localization of ^{3}H-proline at 4 hours after microinjection. The reaction band extends deeper into the enamel and the ameloblasts are still labeled. X 800

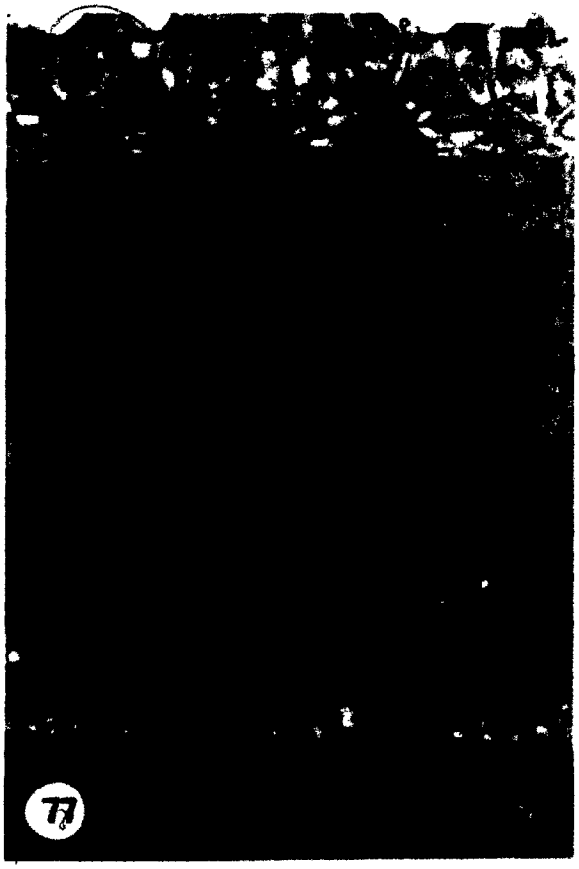
77

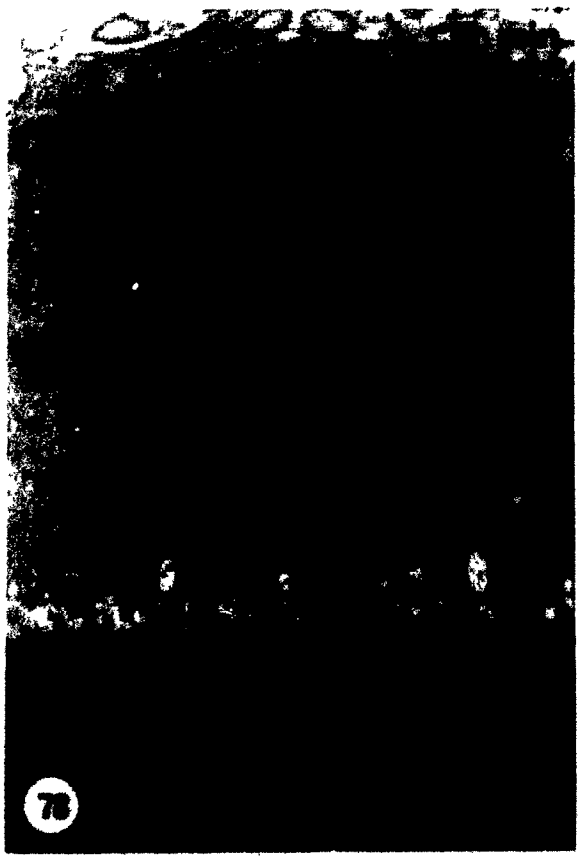
78

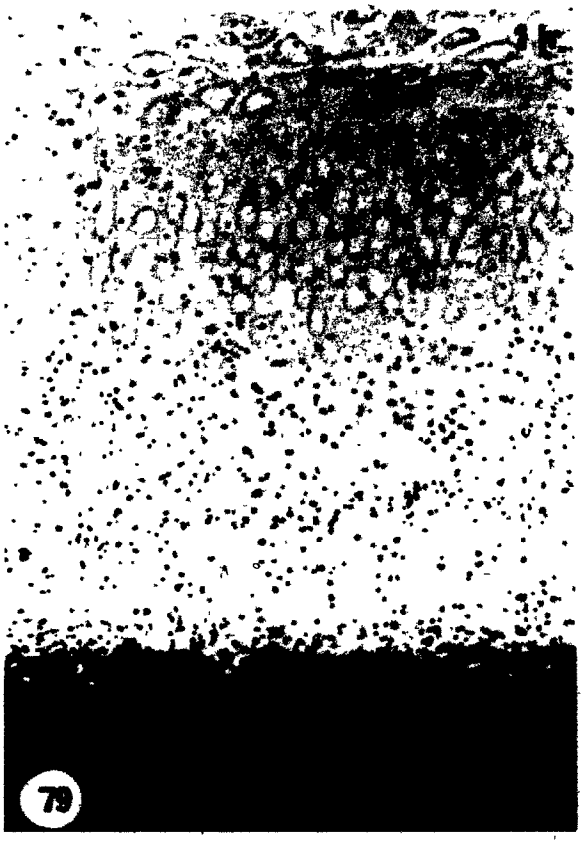
1h
79


4h
80

Figure 81

Radioautographic localization of ^{3}H-proline 1 day after microinjection. The reaction is seen over the entire enamel matrix but stops at the dentino-enamel junction. Some label remains over ameloblasts (AM). EN, enamel. X 800

Figure 82

Radioautographic localization of ^{3}H-proline 2 days after microinjection. The reaction is seen over the entire enamel matrix but little reaction is seen over ameloblasts which have now become ameloblasts of outer enamel secretion. X 600


Pro. 1 d
AM
IN
81


2 d
82

Figure 83

Radioautographic localization of ^{3}H-proline 4 hours after microinjection. This contralateral left hemi-mandible in the same animal as the right hemi-mandible shown in Fig. 80, was not microinjected but shows a reaction band over the predentin. This is presumably due to the systemic circulation of label picked up by the vasculature in the periodontal space. pd, predentin; d, dentin; e, enamel. X 600

Figure 84

Radioautographic localization of ^{3}H-proline 1 day after microinjection. An intense reaction is seen over cells in the connective tissue plug at the drill site and osteoblasts lining an exposed vascular channel (vc) in the alveolar bone (arrowhead). Reactions may be seen in the enamel (large arrow) and over the calcification front of the dentin (small arrow). e, enamel; d, dentin. X 130


Pro 4 h
pd
a


b

Figure 85

Radioautographic localization of ^{125}I-salmon calcitonin 10 minutes after microinjection. Most striking is the reaction seen over the entire enamel matrix (en). Labeling is also seen over ruffle-ended ameloblasts (r-am) and over the periodontal space (ps) but to a lesser extent over the papillary layer (pl). d, dentin. X 400

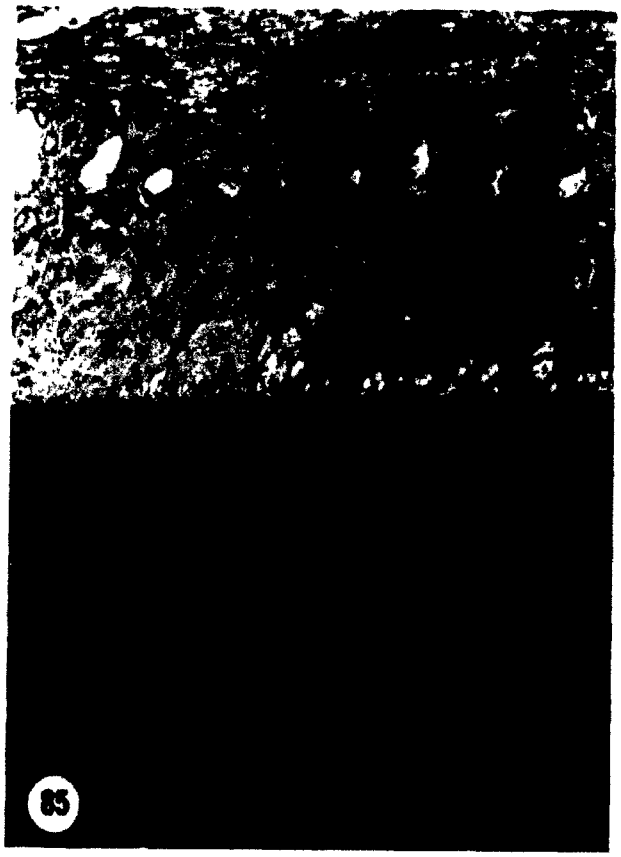
85

Figure 86

Secretory ameloblasts 2 hours after microinjection of vinblastine sulphate. The infranuclear zone (IZ) shows mitochondria (m), rER and numerous secretion granules (arrows). bb, basal bulge. X 9,500

Figure 87

Higher magnification of secretion granules (small arrows) in the infranuclear aone of vinblastine treated ameloblasts. Several secretion granules linked by a continuous membrane may be observed (large arrow). m, mitochondria. X 13,000

Figure 88

Golgi apparatus (G) in the infranuclear zone (IZ) of vinblastine treated ameloblasts. Several secretion granules (arrows) are also seen. X 23,500


VM
86


87


IZ
88

Figure 89

The supranuclear zone (SZ) of secretory ameloblasts 2 h after microinjection of vinblastine sulphate. Accumulations of secretion granules (sg) and a Golgi apparatus (G) are present. Rough endoplasmic reticulum (rER) appears fragmented. Patches of a granular, dark-staining material are seen between ameloblasts (arrows). X 13,500

Figure 90

Higher magnification of Golgi saccules (G) in the supranuclear zone of vinblastine treated ameloblasts. Note the accumulation of secretion granules (sg) near the trans face of the Golgi. X 35,000

Figure 91

Higher magnification of the dark-staining, granular substance (GS) between ameloblasts in vinblastine treated animals. Secretion granules (sg) and coated vesicles (cv) are seen nearby and coated pits (arrows) may be present on the cell membrane. X 36,500

88
89
91

Figure 92

Tomes' processes (TP) of secretory ameloblasts 2 hours after microinjection of vinblastine sulphate. The interdigitating portion of Tomes' process is completely devoid of organelles. A tubular network is sometimes observed (arrows). en, enamel. X 12,000

Figure 93

Tomes' processes (TP) of secretory ameloblasts 2 hours after microinjection of vinblastine sulphate. Occasional membrane infoldings (large arrows) are seen and coated pits (small arrows) are also present. en, enamel. X 15,000


92


TP
93

Figure 94

Lesion in which the dentin deliberately was ruptured by the bur and the animal sacrificed 4 d after drilling. Both the dentin (d) and the enamel (e) are discontinuous along the length of the lesion and dentin fragments (df) may be seen at the ruptured site. Odontoblasts (od) remain active and continue to secrete dentin (large arrows) along the length of the lesion. Where the original dentin still remains, a dark line (small arrows), presumably due to the trauma, separates the pre-drilling dentin from the post-drilling dentin secreted over the 4 day period. Note the similar dark line in the dentin fragment (df). PS, periodontal space; vs, venous sinus. X 120.


vs
4d
94

BIBLIOGRAPHY

BIBLIOGRAPHY

Adams, D. 1962 The blood supply to the enamel organ of the rodent incisor. Archs. Oral Biol., 7: 279-286.

Berkovitz, B.K.B., and R.C. Shore 1978a The ultrastructure of the enamel aspect of the rat incisor periodontium in normal and root-resected teeth. Archs. Oral Biol., 23: 681-689.

Berkovitz, B.K.B., and R.C. Shore 1978b High mitochondrial density within peripheral nerve fibers of the periodontal ligament of the rat incisor. Archs. Oral Biol., 23: 207-213.

Boyde, A. 1969 Electron microscopic observations relating to the nature and development of prism decussation in mammalian dental enamel. Bull. Group. Int. Rech. Sc. Stomat., 12: 151-207.

Carneiro, J., and C.P. Leblond 1959 Role of the osteoblasts and odontoblasts in secreting the collagen of bone and dentin, as shown by radioautography in mice given tritium-labeled glycine. Exp. Cell Res., 18: 291-300.

Chiba, M. 1965 Cellular proliferation in the tooth germs of the rat incisor. Archs. Oral Biol., 10: 707-718.

Dustin, P. 1978 Microtubule Poisons. In: Microtubules. Springer-Verlag.

Ekholm, R., L.E. Ericson, J.O. Josephson and A. Melander 1974 In vivo action of vinblastine on thyroid ultrastructure and hormone secretion. Endocrinol., 94: 641-649.

Elwood, W.K., and M.H. Bernstein 1968 The ultrastructure of the enamel organ related to enamel formation. Am. J. Anat., 122: 73-94.

Ericson, L.E. 1980 Vinblastine-induced inhibition of protein transport in the mouse thyroid in vivo. Endocrinol., 106: 833-841.

Fearnhead, R.W. 1960 Mineralization of rat enamel. Nature, 188: 509-510.

Fearnhead, R.W. 1961a Secretory products of ameloblasts. In: Electron Microscopy in Anatomy. Edward Arnold (Pub.) Ltd., London, pp. 241- 260.

Fearnhead, R.W. 1961b Electron microscopy of forming enamel. Archs. Oral Biol. (Suppl.), 4: 24-28.

Garant, P.R., and R. Gillespie 1969 The presence of fenestrated capillaries in the papillary layer of the enamel organ. Anat. Rec., 163: 71-80.

Garant, P.R., and J. Nalbandian 1968 The fine structure of the papillary region of the mouse enamel organ. Archs. Oral Biol., 13: 1167-1185.

Gould, T.R.L., A.H. Melcher and D.M. Brunette 1977 Location of progenitor cells in periodontal ligament of mouse molar stimulated by wounding. Anat. Rec., 188: 133-142.

Hunter, W.M., and F.C. Greenwood 1962 Preparation of iodine-131 labeled human growth hormone of high specific activity. Nature, 194:495-496.

Hwang, W.S.S., and E.A. Tonna 1965 Autoradiographic analysis of labeling indices and migration rates of cellular components of mouse incisors using tritiated thymidine. J. Dent. Res., 44: 42-53.

Iwaku, F., and H. Ozawa 1979 Blood supply of the rat periodontal space during amelogenesis as studied by the injection replica SEM method. Arch. histol. jap., 42: 81-88.

Josephsen, K., and O. Fejerskov 1977 Ameloblast modulation in the maturation zone of the rat incisor enamel organ. A light and electron microscopic study. J. Anat., 124: 45-70.

Josephsen, K., and H. Warshawsky 1982 Radioautography of rat incisor dentin as a continuous record of the incorporation of a single dose of ^{3}H-labeled proline and tyrosine. Am. J. Anat., 164: 45-56.

Kallenbach, E. 1967 Cell architecture in the papillary layer of rat incisor enamel organ at the stage of enamel maturation. Anat. Rec., 157: 683-698.

Kallenbach, E. 1973 The fine structure of Tomes' process of rat incisor ameloblasts and its relationship to the elaboration of enamel. Tissue Cell, 5: 501-524.

Kallenbach, E. 1980a Fate of horseradish peroxidase in the secretion zone of the rat incisor enamel organ. Tissue Cell, 12: 491-501.

Kallenbach, E. 1980b Access of horseradish peroxidase (HRP) to the extracellular spaces of the maturation zone of the rat incisor enamel organ. Tissue Cell, 12: 165-174.

Kallenbach,E., Y. Clermont and C.P. Leblond 1965 The cell web in the ameloblasts of the rat incisor. Anat. Rec., 153: 55-70.

Kallenbach, E., E. Sandborn and H. Warshawsky 1963 The Golgi apparatus of the ameloblast of the rat at the stage of enamel matrix formation. J. Cell Biol., 16: 629.

Kalnins, Berzins-Raimonds, A. 1949 Changes in tooth and bone tissue produced by placing caps upon incisors of rodents. Amer. J. Orthodont., 35: 219.

Karim, A., and H. Warshawsky 1979 The effect of colcemid on the structure and secretory activity of ameloblasts in the rat incisor as shown by radioautography after injection of ^{3}H-proline. Anat. Rec., 37:587-610.

Kindlova, M., and V. Matena 1959 Blood circulation in the rodent teeth of the rat. Acta Anat., 37: 165-192.

Kinoshita, Y. 1979 Incorporation of serum albumin into the developing dentine and enamel matrix in the rabbit incisor. Calcif. Tissue Int., 29: 41-46.

Kopriwa, B.M., and C.P. Leblond 1962 Improvement in the coating technique for radioautography. J. Histochem. Cytochem., 10: 269-284.

Leblond, C.P., and H. Warshawsky 1979 Dynamics of enamel formation in the rat incisor tooth. J. Dent. Res., 58(B): 950.

Lehner, J., and H. Plenk 1936 Die Zaehne. In: Handbuch der mikroskopischen Anatomie des Menschen. W.V. Moellendorff, ed. Springer, Verlag Berlin. Vol. 5, part 3, 479-490.

Matena, V. 1972 The periodontium of the enamel aspect of the rat incisor. J. Periodont., 43: 311-315.

Melcher, A.H. 1970 Repair of wounds in the periodontium of the rat. Influence of periodontal ligament on osteogenesis. Archs. Oral Biol., 15: 1183-1204.

Moe, H., and H. Mikkelsen 1977 Light microscopical and ultrastructural observations on the effect of vinblastine on ameloblasts of rat incisors in vivo. Acta Path. Microbiol. Scand. Sect. A, 85: 73-88.

Nakagami, K., H. Warshawsky and C.P. Leblond 1971 The elaboration of protein and carbohydrate by rat para thyroid cells as revealed by electron microscope radioautography. J. Cell Biol., 51: 596-610.

Nanci, A. 1982 A morphological study of Tomes' process, enamel matrix and the matrix to crystallite relationship in the rat incisor. Ph. D. Thesis, McGill University, Montreal.

Narayanan, A.S., and R.C. Page 1983 Connective tissues of the periodontium: A summary of current work. Collagen Rel. Res., 3: 33-64.

Ness, A.R., and D.E. Smale 1959 The distribution of mitoses and cells in the tissues bounded by the socket wall of the rabbit mandibular incisor. Proc. Roy. Soc. B., 151: 106-128.

Nishikawa, S., and H. Kitamura 1982 Effect of colcemid on ultrastructure of secretory ameloblast of rat incisor with special reference to microtubules. Jap. J. Oral Biol., 24: 525-528.

Ogura, H., and Y. Kinoshita 1983 The difference in the distribution pattern of administered serum albumin between developing dentine and enamel matrix in the rabbit incisor. In: Mechanisms of Tooth Enamel Formation. Ed. S. Suga. pp. 143-154. Quintessence Publ. Co., Inc.

Okamura, K. 1983 Localization of serum albumin in dentin and enamel. J. Dent. Res., 62: 100-104.

Redman, C.M., D. Banerjee, K. Howell and G.E. Palade 1975 Colchicine inhibition of plasma protein release from rat hepatocytes. J. Cell Biol., 66: 42-59.

Reith, E.J. 1959 The enamel organ of the rat's incisor, its histology and pigment. Anat. Rec., 133: 75-103.

Reith, E.J. 1961 The ultrastructure of ameloblasts during matrix formation and the maturation of enamel. J. Biophys. Cytol., 9:825-840.

Reith, E.J. 1963 The ultrastructure of ameloblasts during early stages of maturation of enamel. J. Cell Biol., 18:691-696.

Reynolds, E.S. 1963 The use of lead citrate at high pH as an electron opaque stain in electron microscopy. J. Cell Biol., 17: 208-212.

Robinson, C., H.D. Briggs, P.J. Atkinson and J.A. Weatherell 1981 Chemical changes during formation and maturation of human deciduous enamel. Archs. Oral Biol., 26: 1027-1033.

Robinson, C., P. Fuchs, D. Deutsch and J.A. Weatherell 1978 Four chemically distinct stages in developing enamel from bovine incisor teeth. Caries Res., 12: 1 -11.

Robinson, C., N.R. Lowe and J.A. Weatherell 1977 Changes in amino acid compostion of developing rat incisor enamel. Calcif. Tiss. Res., 23: 19-21.

Ronnholm, E. 1962 An electron microscope study of amelogenesis in human teeth. I. The fine structure of ameloblasts. J. Ultrastructure Res., 6: 229-248.

Skobe, Z. 1976 The secretory stage of amelogenesis in the rat mandibular incisor teeth observed by scanning electron microscopy. Calcif. Tiss. Res., 21: 83-103.

Skobe, Z. 1980 Scanning electron microscopy of the mouse incisor enamel organ in transition between secretory and maturation stages of amelogenesis. Archs. Oral Biol., 25: 395-401.

Skobe, Z., and P.R. Garant 1974 Electron microscopy of horseradish peroxidase uptake by papillary cells of the mouse incisor enamel organ. Archs. Oral Biol., 19: 387-395.

Smith, C.E. 1979 Ameloblasts: Secretory and resorptive functions. J. Dent. Res., 58(B): 605-706.

Smith, C.E., and H. Warshawsky 1975 Cellular renewal in the enamel organ and the ameloblast layer of the rat incisor as followed by radioautography using ^{3}H-thymidine. Anat. Rec., 183: 523-562.

Smith, C.E., and H. Warshawsky 1977 Quantitative analysis of cell turnover in the enamel organ ofthe rat incisor. Evidence for ameloblast death immediately after enamel matrix secretion. Anat. Rec., 187: 63-97.

Starkey, W.E. 1963 The migration and renewal of tritium labeled cells in the developing enamel organs of rabbits. Brit. Dent. J., 115:143-153.

Takano, Y., and M. Crenshaw 1979 The penetration of intravascularly perfused lanthanum into develpoing rat molar teeth. IADR Progr. and Abst. 58: No. 362.

Takuma, S., T. Sawada and T. Yanagisawa 1982 Ultrastructural changes of secreting rat-incisor ameloblasts following administration of vincristine and vinblastine. J. Dent. Res., 61 (Sp. Iss.):1472-1478.

Tomes, J. 1850 On the structure of the dental tissues of the order Rodentia. Philos. Trans. Roy. Soc. London, 140: 529-548.

Watson, M.L. 1958 Staining tissue sections for electron microscopy with heavy metals. J. Biophys. Biochem. Cytol., 4: 475.

Watson, M.L. 1960 The extracellular nature of enamel in the rat. J. Biophys. Biochem. Cytol., 7: 489-492.

Watson, M.L., and J.K. Avery 1954 The development of the hamster lower incisors as observed by electron microscopy. Am. J. Anat., 95:109-161.

Warshawsky, H. 1966 The formation of enamel matrix proteins. Ph. D. Thesis, McGill University, Montreal.

Warshawsky, H. 1968 The fine structure of secretory ameloblasts in rat incisors. Anat. Rec., 161:211-229.

Warshawsky, H. 1971 A light and electron microscopic study of the nearly mature enamel of rat incisors. Anat. Rec., 169: 559-584.

Warshawsky, H. 1978 A freeze-fracture study of the topographic relationship between inner enamel-secretory ameloblasts in the rat incisor. Am. J. Anat., 152: 153-208.

Warshawsky, H. 1979 Radioautographic studies on amelogenesis. J. Biol. Buccale, 7: 105-126.

Warshawsky, H., K. Josephsen, A. Thylstrup and O. Fejerskov 1981 The development of enamel structure in rat incisors as compared to the teeth of monkey and man. Anat. Rec., 200: 371-399.

Warshawsky, H., and G. Moore 1967 A technique for the fixation and decalcification of rat incisors for electron microscopy. J. Histochem. Cytochem., 15: 543-549.

Warshawsky, H., and C.E. Smith 1971 A three-dimensional reconstruction of the rods in rat maxillary incisor enamel. Anat. Rec., 169:585-592.

Warshawsky, H., and C.E. Smith 1974 Morphological classification of rat incisor ameloblasts. Anat. Rec., 188: 143-172.

Warshawsky, H., and I. Vugman 1977 A comparison of the protein synthetic activity of presecretory and secretory ameloblasts in rat incisors. Anat. Rec., 188: 143-172.

Weinstock, A., and C.P. Leblond 1971 Elaboration of the matrix glycoprotein of enamel by the secretory ameloblasts of the rat incisor as revealed by radioautography after galactose-^{3}H injection. J. Cell Biol., 51: 26-51.

Weinstock, M., and C.P. Leblond 1974 Synthesis, migration, and release of precursor collagen by odontoblasts as visualized by radioautography after ^{3}H-proline administration. J. Cell Biol., 60: 92-127.

Williams, J.A. 1981 Effects of anti-mitotic agents on ultrastructure and intracellular transport of protein in pancreatic acini. In: Basic Mechanisms of Cellular Secretion; Hand, A.R. and C. Oliver (eds.). Methods in Cell Biol., 23: 247-258.

Williams, J.L. 1896 On the formation and structure of dental enamel. Dental Cosmos., 38: 101-127.

Young, R.W., and R.C. Greulich 1963 Distinctive autoradiographic patterns of glycine incorporation in rat enamel and dentine matrices. Archs. Oral Biol., 8: 509-521.